

European Research Council



JOHANNES GUTENBERG  
UNIVERSITÄT MAINZ

INSTITUTE  
FOR GEOSCIENCES  
GEOPHYSICS AND GEODYNAMICS



# A parallel modeling tool for lithospheric deformation

Anton Popov, Boris Kaus, Tobias Baumann, Adina Püsök, Georg Reuber

JGU-Mainz

Schloss Schney, Lichtenfels 2016

# LaMEM Lithosphere and Mantle Evolution Model FDSTAG Code



European Research Council



Johannes Gutenberg  
Universität Mainz



JUQUEEN - Jülich Blue Gene/Q



P Portable,  
E Extensible  
T Toolkit for  
S Scientific  
C Computation

# Outline

Introduction

FDSTAG discretization

Nonlinear rheology

Analytical Jacobian

Multigrid and scaling

Stress rates

Plasticity convergence

Conservative velocity interpolation

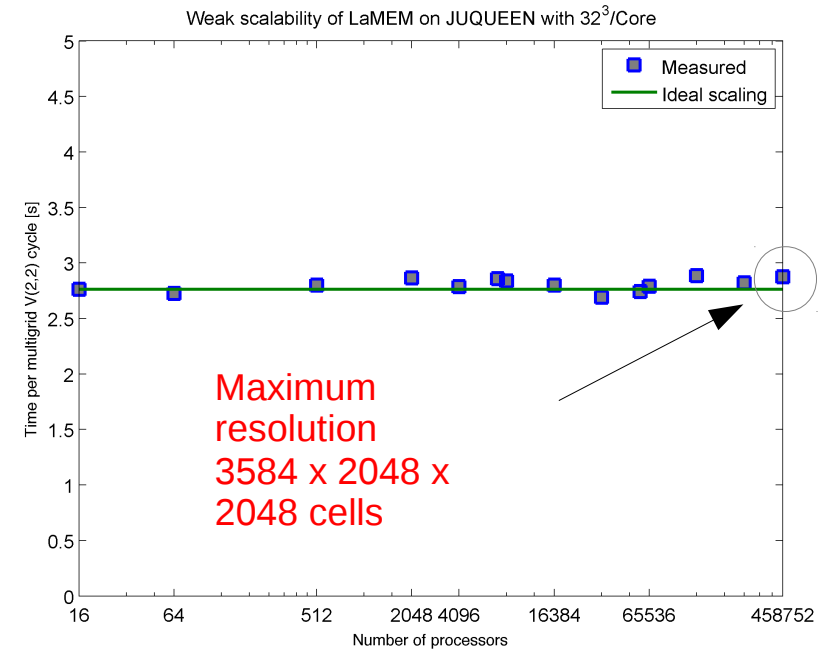
Adjoint gradients and inversion

Adjoint scaling laws

Other inversion techniques and examples

# LaMEM (Lithosphere and Mantle Evolution Model)

- 3D thermo-mechanical code, written in C uses PETSc.
- Nonlinear visco-elasto-plastic rheologies
- Runs on 1-458'752 processors routinely on 1024-4096
- Current version of code only supports staggered difference method (faster than FE)
- Can use a large variety of (multigrid) solvers (Galerkin GMG, AMG, Coupled/decoupled)
- Marker-and-cell method, free surface, (coupled to erosion model)
- Polygonal meshes to create (complex) input geometries.





# https://bitbucket.org/bkaus/lamem

Atlassian **Bitbucket** Features Pricing

Find a repository... English Sign up Log in

**C** LaMEM

**ACTIONS**

- Clone
- Compare
- Fork

**NAVIGATION**

- Overview
- Source
- Commits
- Branches
- Pull requests
- Downloads

Boris Kaus / LaMEM

## Overview

Last updated	2016-09-06	12	0
Language	C	Branches	Tags
Access level	Read	0	11
		Forks	Watchers

```
=====
LaMEM - Lithosphere and Mantle Evolution Model

A parallel 3D numerical code that can be used to model various thermomechanical
geodynamical processes such as mantle-lithosphere interaction for rocks
that have visco-elasto-plastic rheologies. The code is build on top of
PETSc and the current version of the code uses a marker-in-cell
approach with a staggered finite difference discretization.

A range of (Galerkin) multigrid and iterative solvers are
available, for both linear and non-linear rheologies, using Picard and
quasi-Newton solvers (provided through the PETSc interface).

LaMEM has been tested on over 458'000 cores.

The current version is developed by
Anton Popov (Johannes Gutenberg University Mainz, popov@uni-mainz.de), 2011-
Boris Kaus (JGU Mainz, kaus@uni-mainz.de), 2011-
Tobias Baumann (JGU Mainz), 2011-
Adina Püsök (JGU Mainz), 2012-
Naiara Fernandez (JGU Mainz), 2011-2014
Arthur Bauville (JGU Mainz), 2015

Older versions of LaMEM included a finite element solver as well,
and were developed by:
```

HTTPS <https://bitbucket.org/bkaus/lamem>

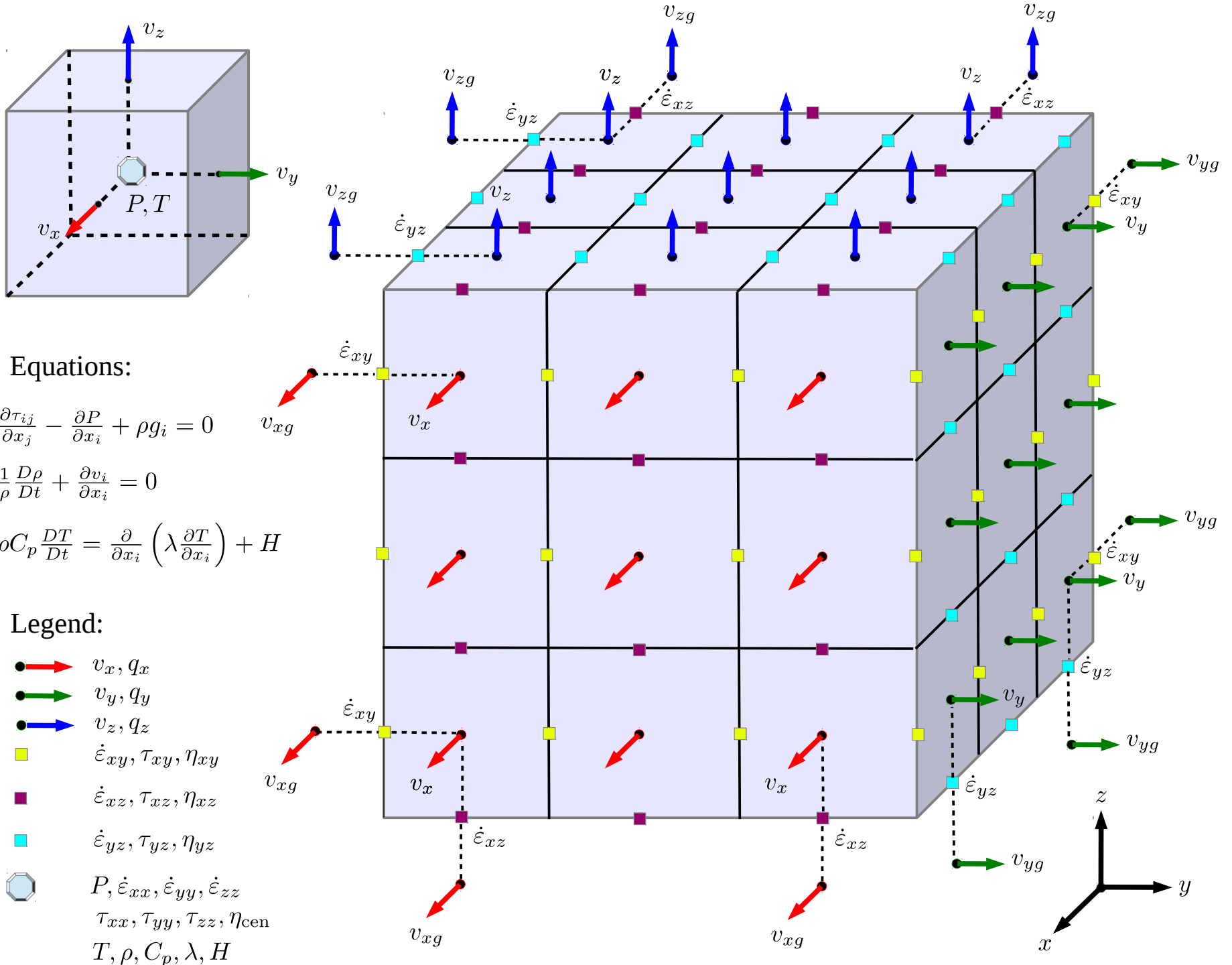
Unlimited private and public hosted repositories. Free for small teams!

[Sign up for free](#)

**Recent activity**

- 1 commit**  
Pushed to bkaus/lamem  
[c53180e](#) tentative solution for correct pres...  
lapopov · 2016-09-06
- 1 commit**  
Pushed to bkaus/lamem  
[8126763](#) Input file  
Beatriz Martinez Montesinos · 2016-09-06
- 2 commits**  
Pushed to bkaus/lamem  
[158e40c](#) Merge branch 'explicit' of <https://...>  
[ef9532d](#) First changes for density scaling  
Beatriz Martinez Montesinos · 2016-09-06
- 1 commit**  
Pushed to bkaus/lamem  
[379d3ee](#) Merge remote-tracking branch 'o...  
Boris Kaus · 2016-09-04

# Parallel staggered grid layout implementation



# Parallel staggered grid layout implementation

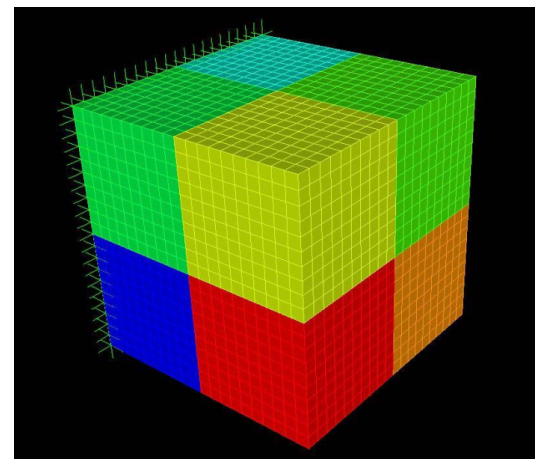
## PETSc Distributed Array (DMDA)

- Parallel (MPI) each processor owns its local part of the grid
- Natural I-J-K indexing (global indices)!
- Local vectors with ghost points
- Boundary ghost points
- Global distributed vectors w/o ghost points
- Local to Global scatter/assembly operations

Altogether 8 DMDA objects are used

Corner DMDA is used for ParaView output

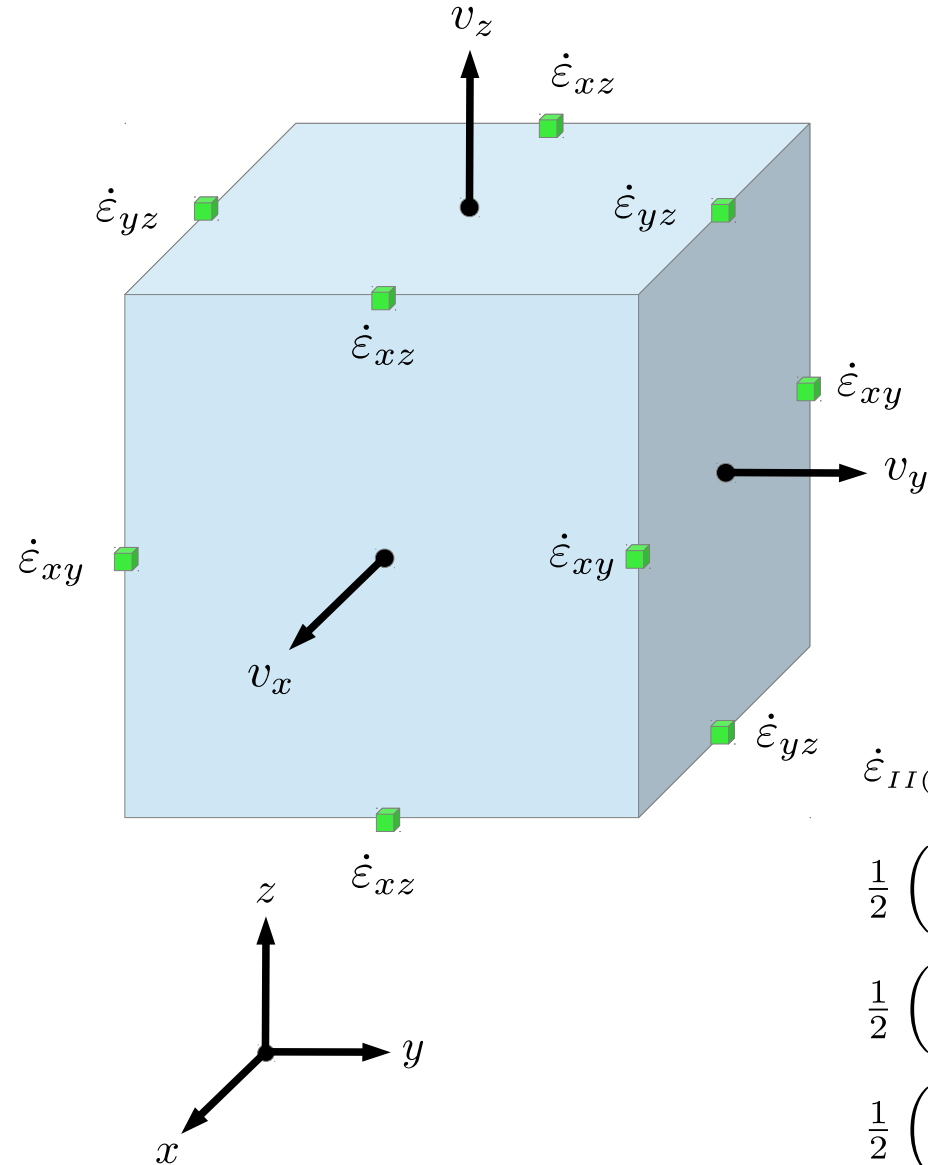
Coordinates are stored in local 1D arrays since grid is rectilinear



NAME	x-size	y-size	z-size	Ghost points
DA_CORNER	Nx	Ny	Nz	None
DA_CENTER	Nx - 1	Ny - 1	Nz - 1	All
DA_XY	Nx	Ny	Nz - 1	None
DA_XZ	Nx	Ny - 1	Nz	None
DA_YZ	Nx - 1	Ny	Nz	None
DA_X	Nx	Ny - 1	Nz - 1	Y & Z
DA_Y	Nx - 1	Ny	Nz - 1	X & Z
DA_Z	Nx - 1	Ny - 1	Nz	X & Y

# Nonlinear terms discretization

Example: interpolation scheme for the central points



There are three set of edge points:  
XY, XZ and YZ, defining corresponding  
shear strain rates:

$$\dot{\epsilon}_{xy}, \dot{\epsilon}_{xz}, \dot{\epsilon}_{yz}$$

Central point defines normal strain rates:

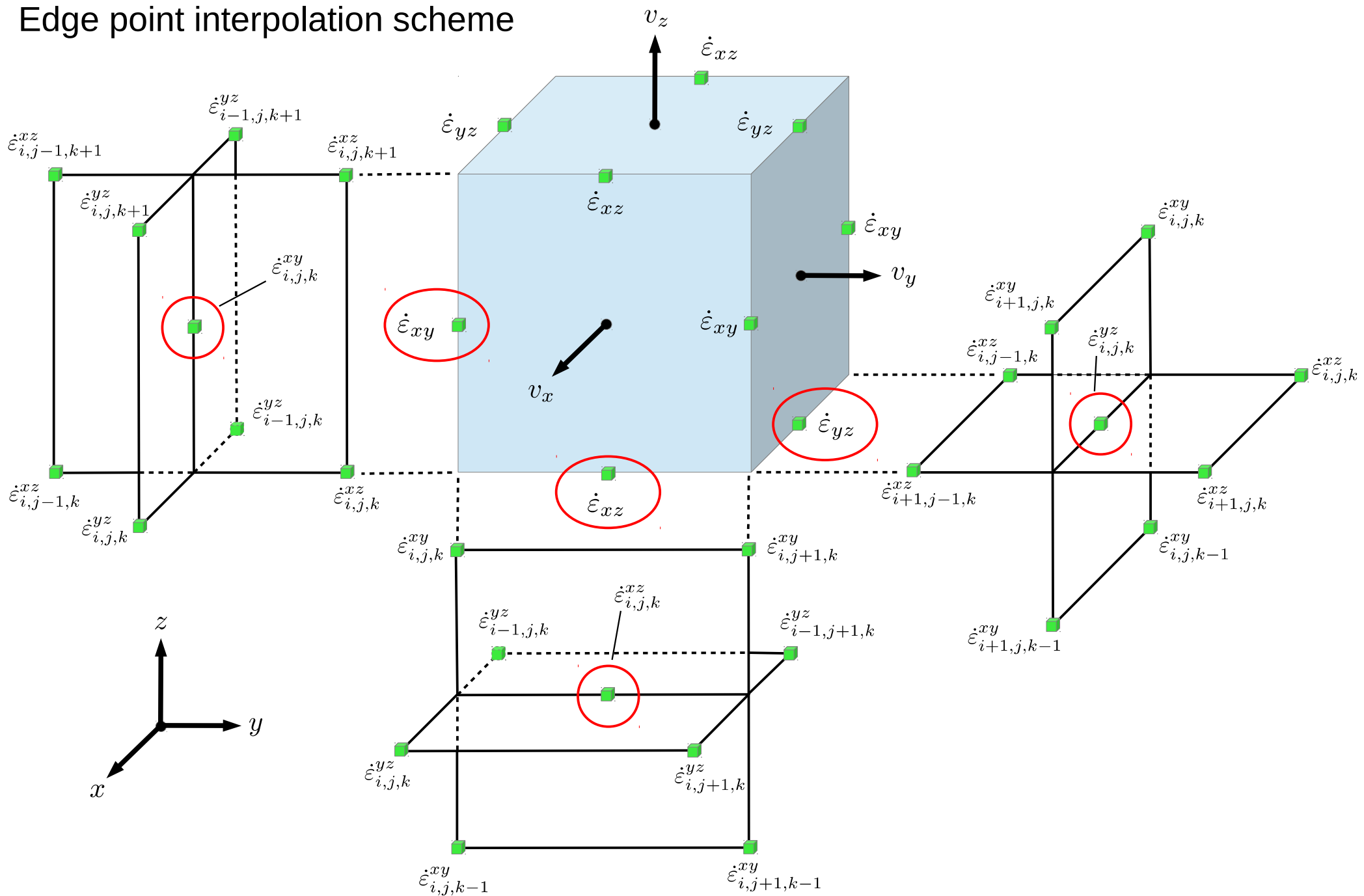
$$\dot{\epsilon}_{xx}, \dot{\epsilon}_{yy}, \dot{\epsilon}_{zz}$$

Second invariant discretization:

$$\begin{aligned} \dot{\epsilon}_{II(i,j,k)} = & \dot{\epsilon}_{xx(i,j,k)}^2 + \dot{\epsilon}_{yy(i,j,k)}^2 + \dot{\epsilon}_{zz(i,j,k)}^2 + \\ & \frac{1}{2} \left( \dot{\epsilon}_{xy(i,j,k)}^2 + \dot{\epsilon}_{xy(i,j+1,k)}^2 + \dot{\epsilon}_{xy(i+1,j,k)}^2 + \dot{\epsilon}_{xy(i+1,j+1,k)}^2 \right) + \\ & \frac{1}{2} \left( \dot{\epsilon}_{xz(i,j,k)}^2 + \dot{\epsilon}_{xz(i,j,k+1)}^2 + \dot{\epsilon}_{xz(i+1,j,k)}^2 + \dot{\epsilon}_{xz(i+1,j,k+1)}^2 \right) + \\ & \frac{1}{2} \left( \dot{\epsilon}_{yz(i,j,k)}^2 + \dot{\epsilon}_{yz(i,j,k+1)}^2 + \dot{\epsilon}_{yz(i,j+1,k)}^2 + \dot{\epsilon}_{yz(i,j+1,k+1)}^2 \right) \end{aligned}$$

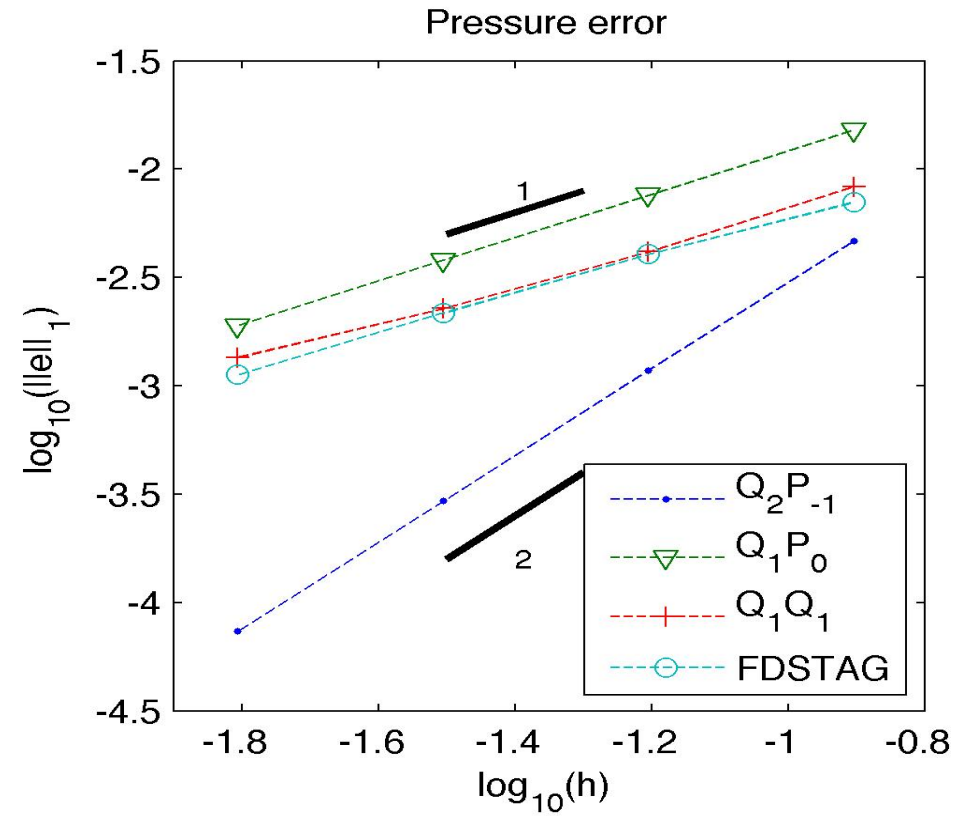
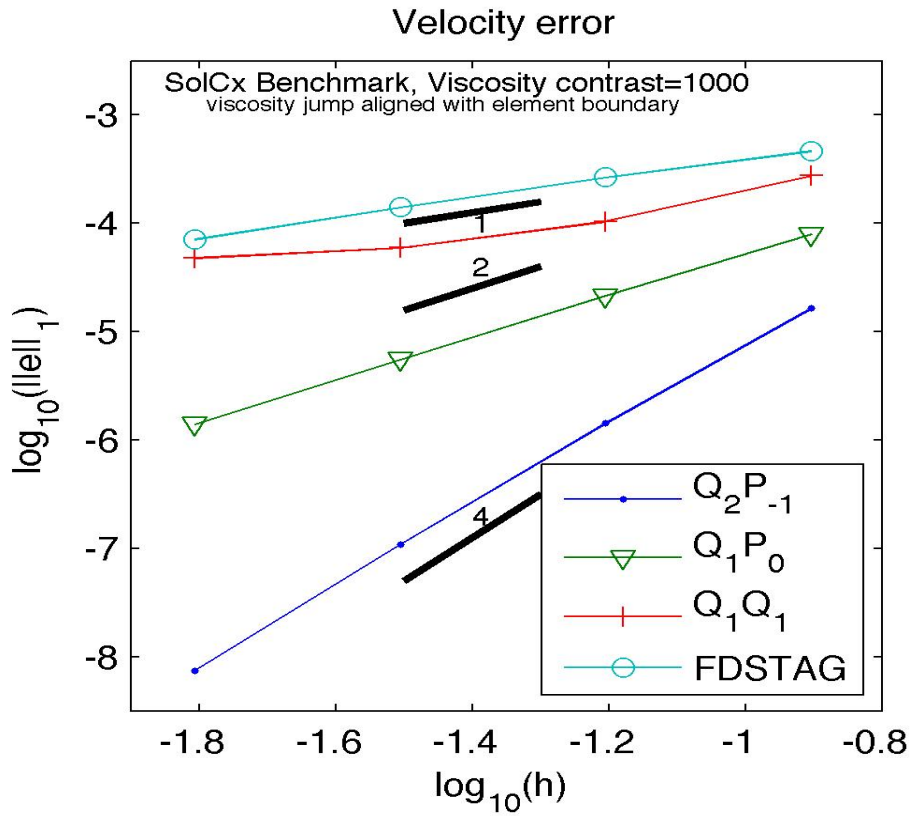
# Nonlinear terms discretization

Edge point interpolation scheme



# FDSTAG vs. FE convergence (SolCx benchmark)

Viscosity contrast 1000, element boundary aligned with jump

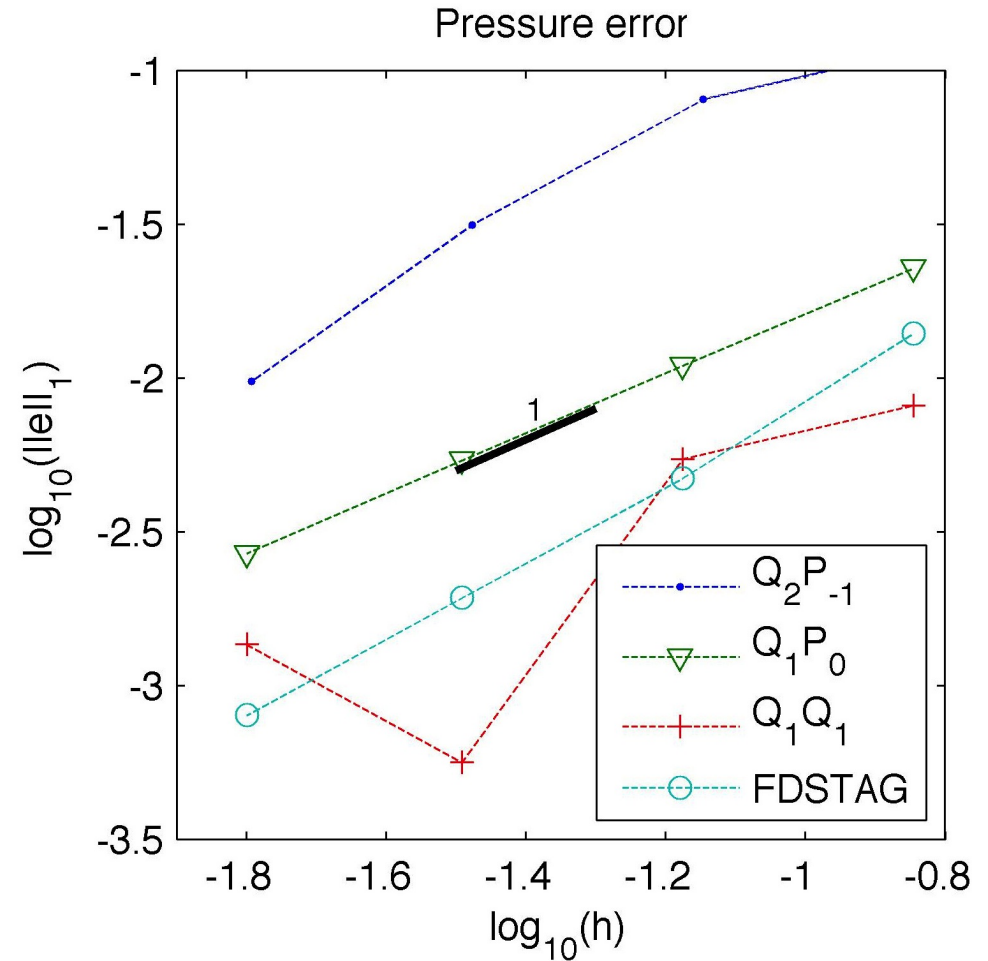
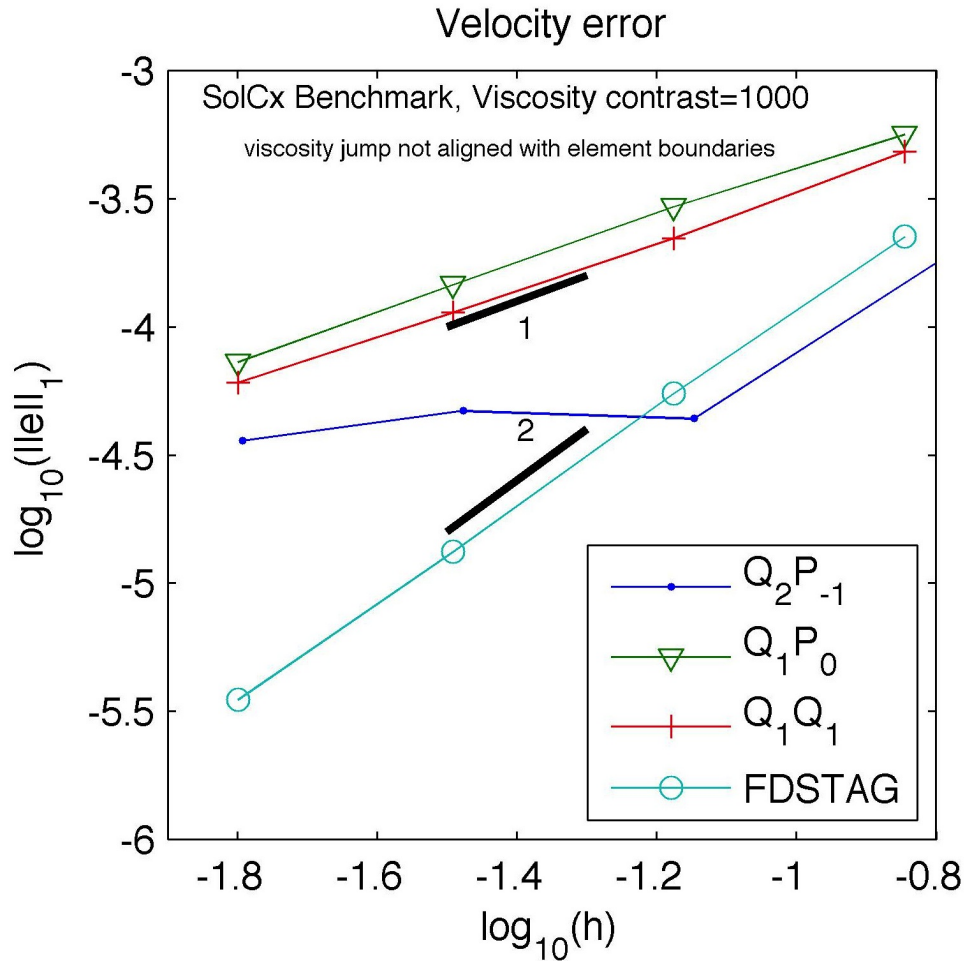


High-order element wins



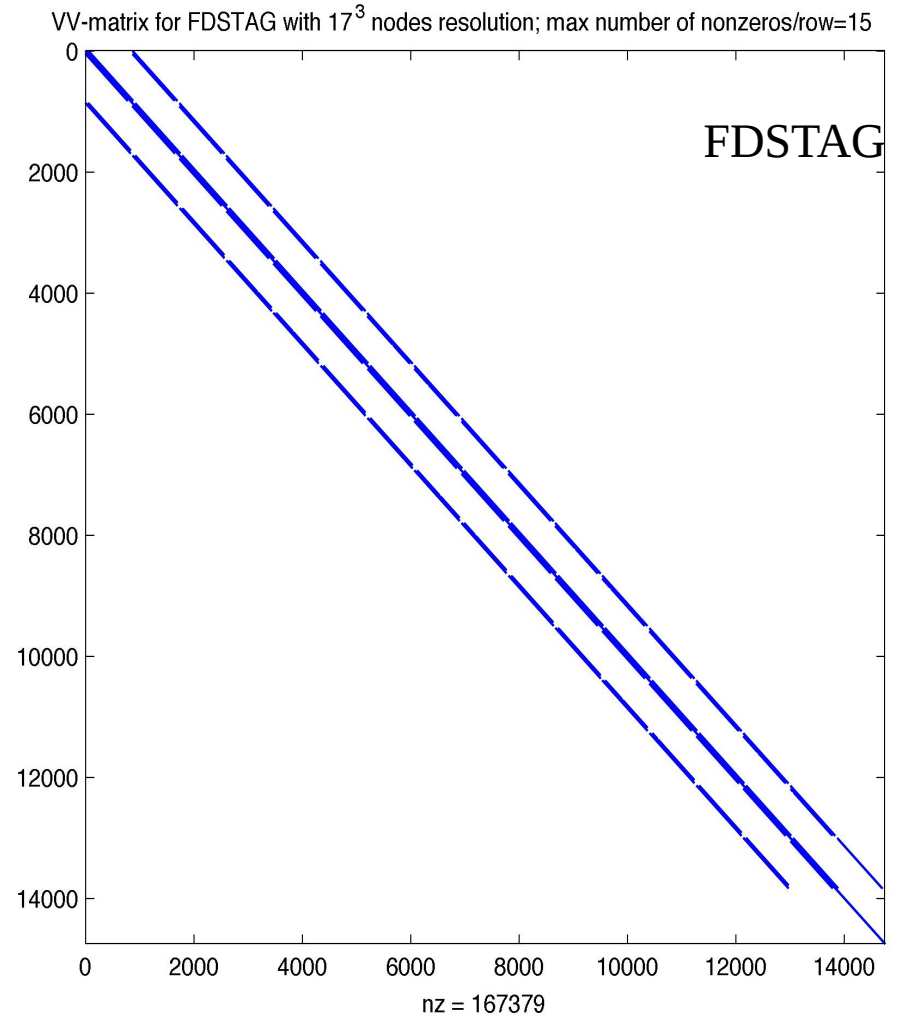
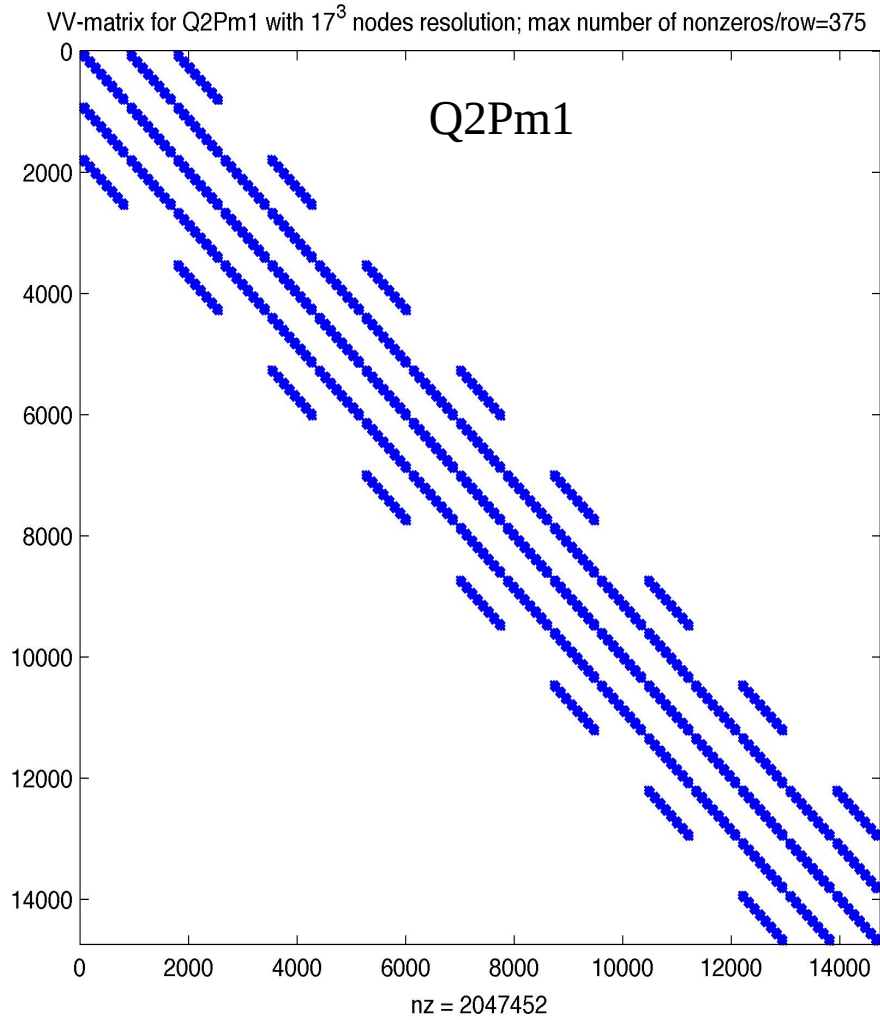
# FDSTAG vs. FE convergence (SolCx benchmark)

Viscosity contrast 1000, element boundary NOT aligned with jump



FDSTAG is not so bad  
High-order element fails

# FDSTAG vs. FE memory footprint



FDSTAG requires *significantly* less memory!  
Matrix-vector multiplications are much faster!

# Nonlinear viso-elasto-plastic rheology

Stress update

$$\tau_{ij} = 2\eta^* \dot{\epsilon}_{ij}^*$$

Effective strain rate and invariant

$$\dot{\epsilon}_{ij}^* = \dot{\epsilon}_{ij} + \frac{\tau_{ij}^*}{2G\Delta t} \quad \dot{\epsilon}_{II}^* = \left(\frac{1}{2}\dot{\epsilon}_{ij}^* \dot{\epsilon}_{ij}^*\right)^{1/2}$$

Stress rotation terms (incremental stress rotation as described later)

$$\tau_{ij}^* = \tau_{ij}^n + \Delta t (w_{ik} \tau_{kj}^n - \tau_{ik}^n w_{kj})$$

Deviatoric strain rate

$$\dot{\epsilon}_{ij} = \frac{1}{2} \left( \frac{\partial v_i}{\partial x_j} + \frac{\partial v_j}{\partial x_i} \right) - \frac{1}{3} \frac{\partial v_k}{\partial x_k} \delta_{ij}$$

Spin tensor

$$\omega_{ij} = \frac{1}{2} \left( \frac{\partial v_i}{\partial x_j} - \frac{\partial v_j}{\partial x_i} \right)$$

Effective viscosity

$$\eta^* = \min \left[ \left( \frac{1}{G\Delta t} + \frac{1}{\eta_l} + \frac{1}{\eta_n} + \frac{1}{\eta_p} \right)^{-1}, \frac{\tau_Y}{2\dot{\epsilon}_{II}^*} \right]$$

# Nonlinear visco-elasto-plastic rheology

Drucker-Prager yield stress

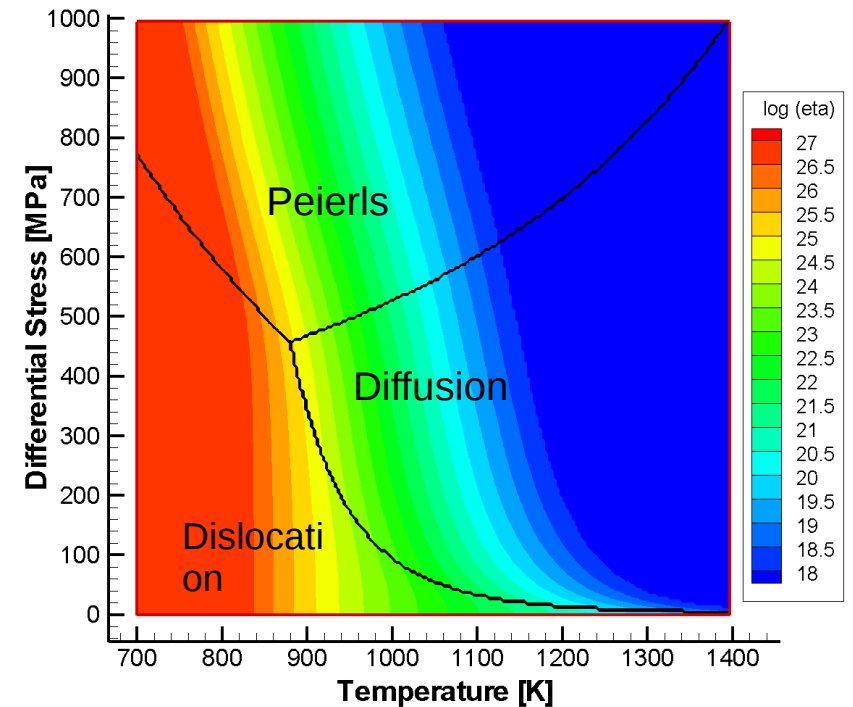
$$\tau_Y = \mu P + c$$

Diffusion Dislocation and Peierls constants

$$A_l = B_l \exp \left[ -\frac{E_l + pV_l}{RT} \right],$$

$$A_n = B_n \exp \left[ -\frac{E_n + pV_n}{RT} \right]$$

$$A_p = \frac{B_p}{(\gamma\tau_p)^s} \exp \left[ -\frac{E_p + pV_p}{RT} (1 - \gamma)^q \right]$$



Effective creep viscosities

$$\eta_l = \frac{1}{2} (A_l)^{-1}$$

$$\eta_n = \frac{1}{2} (A_n)^{-\frac{1}{n}} (\dot{\epsilon}_{II}^*)^{\frac{1}{n}-1}$$

$$\eta_p = \frac{1}{2} (A_p)^{-\frac{1}{s}} (\dot{\epsilon}_{II}^*)^{\frac{1}{s}-1}$$

Peierls effective exponent

$$s = \frac{E_p + pV_p}{RT} (1 - \gamma)^{q-1} q \gamma$$

# Global nonlinear iterations

Preconditioned Newton iteration with line search

$$P^{-1} J(x_k) \delta x_k = -P^{-1} r(x_k) \quad x_{k+1} = x_k + \alpha \delta x_k$$

Jacobian and residual

$$J = \begin{pmatrix} \frac{\partial r_M}{\partial v} & \frac{\partial r_M}{\partial P} & \frac{\partial r_M}{\partial T} \\ \frac{\partial r_C}{\partial v} & \frac{\partial r_C}{\partial P} & \frac{\partial r_C}{\partial T} \\ \frac{\partial r_E}{\partial v} & \frac{\partial r_E}{\partial P} & \frac{\partial r_E}{\partial T} \end{pmatrix} \quad r = \begin{pmatrix} r_M \\ r_C \\ r_E \end{pmatrix} \quad \begin{array}{l} \text{Momentum} \\ \text{Continuity} \\ \text{Energy} \end{array} \quad x = \begin{pmatrix} v \\ P \\ T \end{pmatrix} \quad \begin{array}{l} \text{Velocity} \\ \text{Pressure} \\ \text{Temperature} \end{array}$$

Jacobian-Free-Newton-Krylov (**JFNK**) or analytical matrix-free Jacobian

$$Jy \approx \frac{r(x + hy) - r(x)}{h} \quad \text{-snes\_mf\_operator (PETSc **SNES** solver)}$$

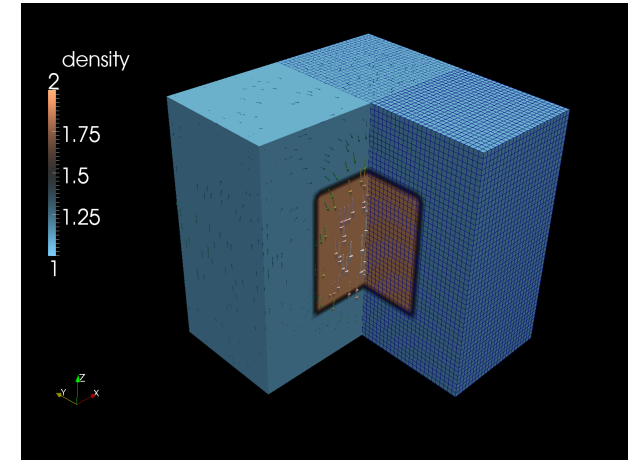
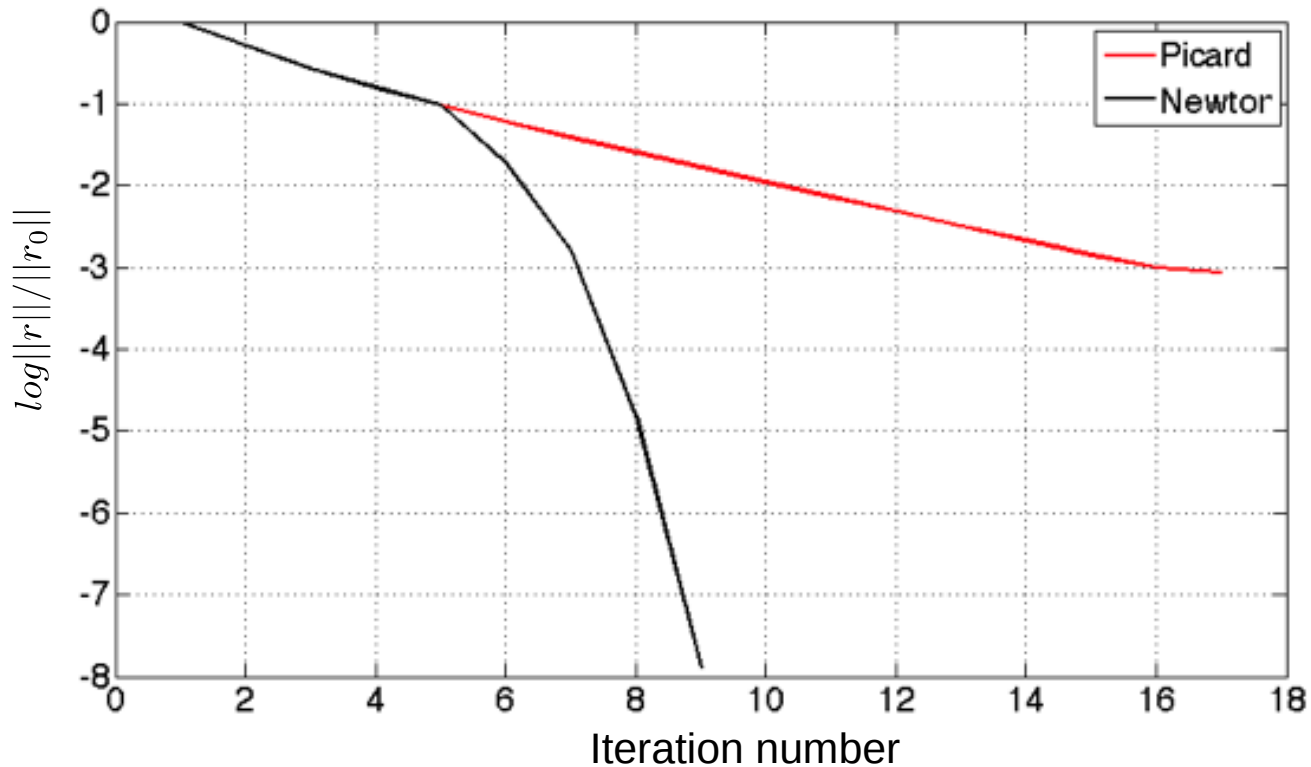
Preconditioner matrix

$$P = \begin{pmatrix} K & G & 0 \\ D & C & 0 \\ 0 & 0 & E \end{pmatrix}$$

# Picard vs. Newton

Quasi-linear residual form:  $r(x) = A(x)x - b = 0$

Picard fixed-point iteration:  $J(x) \approx A(x)$



Picard approximation facilitates convergence at the initial stages

Switching to Picard can improve Newton convergence



# Analytical Jacobian Finite Elements

Nonlinear residuals

$$r^U = \int_{\Omega} B^T (\tau - mP) - N_U^T \rho g \, d\Omega$$

$$r^P = - \int_{\Omega} N_P^T m^T \dot{\varepsilon} \, d\Omega$$

Jacobian iteration

$$\begin{bmatrix} \Delta U_k \\ \Delta P_k \end{bmatrix} = - \begin{bmatrix} J^{UU} & J^{UP} \\ J^{PU} & 0 \end{bmatrix}^{-1} \begin{bmatrix} r_k^U \\ r_k^P \end{bmatrix}$$

$$\begin{bmatrix} U_{k+1} \\ P_{k+1} \end{bmatrix} = \begin{bmatrix} U_k \\ P_k \end{bmatrix} + \alpha \begin{bmatrix} \Delta U_k \\ \Delta P_k \end{bmatrix}$$

Stress and strain rate vectors

$$\begin{aligned} \dot{\varepsilon} &= [\dot{\varepsilon}_{xx} \dot{\varepsilon}_{yy} \dot{\varepsilon}_{zz} \dot{\gamma}_{xy} \dot{\gamma}_{xz} \dot{\gamma}_{yz}]^T \\ \underline{\dot{\varepsilon}} &= [\dot{\varepsilon}_{xx} \dot{\varepsilon}_{yy} \dot{\varepsilon}_{zz} \dot{\varepsilon}_{xy} \dot{\varepsilon}_{yx} \dot{\varepsilon}_{xz} \dot{\varepsilon}_{zx} \dot{\varepsilon}_{yz} \dot{\varepsilon}_{zy}]^T \\ \tau &= [\tau_{xx} \tau_{yy} \tau_{zz} \tau_{xy} \tau_{xz} \tau_{yz}]^T \\ \underline{\tau} &= [\tau_{xx} \tau_{yy} \tau_{zz} \tau_{xy} \tau_{yx} \tau_{xz} \tau_{zx} \tau_{yz} \tau_{zy}]^T \end{aligned}$$

Projection matrix and projection

$$Q = \frac{1}{2} \begin{bmatrix} 2 & 0 & 0 & 0 & 0 & 0 & 0 & 0 & 0 \\ 0 & 2 & 0 & 0 & 0 & 0 & 0 & 0 & 0 \\ 0 & 0 & 2 & 0 & 0 & 0 & 0 & 0 & 0 \\ 0 & 0 & 0 & 1 & 1 & 0 & 0 & 0 & 0 \\ 0 & 0 & 0 & 0 & 0 & 1 & 1 & 0 & 0 \\ 0 & 0 & 0 & 0 & 0 & 0 & 0 & 1 & 1 \end{bmatrix}$$

$$\tau = Q \underline{\tau}, \quad \underline{\dot{\varepsilon}} = Q^T \dot{\varepsilon}$$

Pressure projection vector

$$m = [1 \ 1 \ 1 \ 0 \ 0 \ 0 \ 0 \ 0 \ 0]^T$$

# Analytical Jacobian Finite Elements

Jacobian blocks

$$J^{UU} = \int_{\Omega} B^T Q T Q^T B d\Omega$$

$$J^{UP} = - \int_{\Omega} B^T (m - \mu Q \underline{q}) N_P d\Omega$$

$$J^{PU} = - \int_{\Omega} N_P^T m^T B d\Omega$$

Tangent matrix

$$T = 2\eta^* (I + \beta \underline{q} \underline{q}^T)$$

Visco-elastic nonlinear parameter

$$\beta = \frac{1}{2} \left( \frac{1}{n} - 1 \right) \frac{\eta^*}{\eta_n} + \frac{1}{2} \left( \frac{1}{s} - 1 \right) \frac{\eta^*}{\eta_p}$$

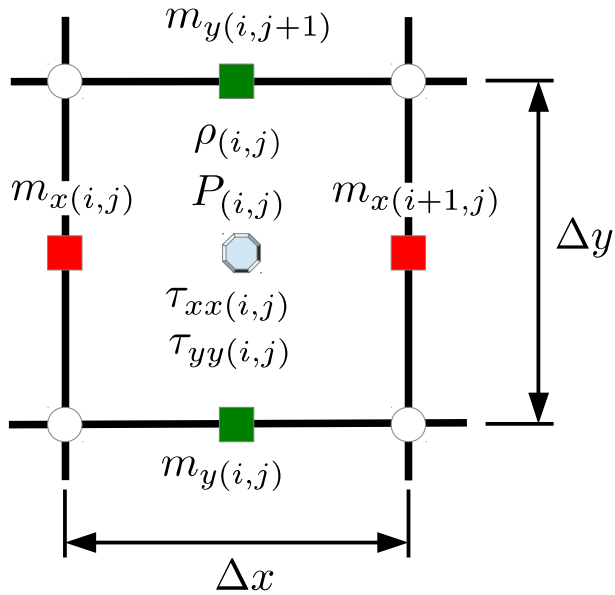
Plastic nonlinear parameter

$$\beta = -\frac{1}{2}$$

Normalized flow vector

$$\underline{q} = \frac{\dot{\underline{\epsilon}}}{\dot{\epsilon}_{II}^*}$$

# Analytical Jacobian Finite Difference (example)



Momentum residual contributions

$$\Delta m_{x(i,j)} = + \frac{\tau_{xx(i,j)} - P(i,j)}{\Delta x} + \frac{1}{2} \rho(i,j) g_x$$

$$\Delta m_{x(i+1,j)} = - \frac{\tau_{xx(i,j)} - P(i,j)}{\Delta x} + \frac{1}{2} \rho(i,j) g_x$$

Residual derivatives (velocity)

$$\frac{\partial \Delta m_{x(i,j)}}{\partial \mathbf{v}} = + \frac{1}{\Delta x} \frac{\partial \tau_{xx(i,j)}}{\partial \mathbf{v}}$$

$$\frac{\partial \Delta m_{x(i+1,j)}}{\partial \mathbf{v}} = - \frac{1}{\Delta x} \frac{\partial \tau_{xx(i,j)}}{\partial \mathbf{v}}$$

Residual derivatives (pressure)

$$\frac{\partial \Delta m_{x(i,j)}}{\partial P} = + \frac{1}{\Delta x} \frac{\partial \tau_{xx(i,j)}}{\partial P} - \frac{1}{\Delta x}$$

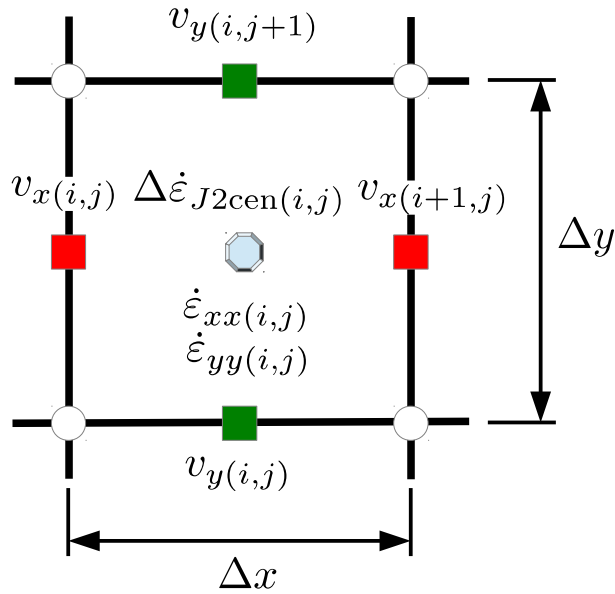
$$\frac{\partial \Delta m_{x(i+1,j)}}{\partial P} = - \frac{1}{\Delta x} \frac{\partial \tau_{xx(i,j)}}{\partial P} + \frac{1}{\Delta x}$$

Stress derivatives

$$\frac{\partial \tau_{xx(i,j)}}{\partial \mathbf{v}} = 2 \frac{\partial \eta_{\text{cen}}^*(i,j)}{\partial \mathbf{v}} \dot{\epsilon}_{xx}^*(i,j) + 2 \eta_{\text{cen}}^*(i,j) \frac{\dot{\epsilon}_{xx}^*(i,j)}{\partial \mathbf{v}}$$

$$\frac{\partial \tau_{xx(i,j)}}{\partial P} = \mu \frac{\dot{\epsilon}_{xx}^*(i,j)}{\dot{\epsilon}_{II}^*}$$

# Analytical Jacobian Finite Difference (example)



Viscosity derivatives

$$\frac{\partial \eta^*}{\partial \mathbf{v}} = \frac{\partial \eta^*}{\partial \dot{\epsilon}_{II}} \frac{\partial \dot{\epsilon}_{II}}{\partial \dot{\epsilon}_{J2}} \frac{\partial \dot{\epsilon}_{J2}}{\partial \mathbf{v}} \quad \frac{\partial \dot{\epsilon}_{II}}{\partial \dot{\epsilon}_{J2}} = \frac{1}{2} (\dot{\epsilon}_{II})^{-1}$$

$$\frac{\partial \eta^*}{\partial \dot{\epsilon}_{II}} = \left( \frac{\eta^*}{\eta_n} \right)^2 \left( \frac{1}{n} - 1 \right) \frac{\eta_n}{\dot{\epsilon}_{II}^*} + \left( \frac{\eta^*}{\eta_p} \right)^2 \left( \frac{1}{s} - 1 \right) \frac{\eta_p}{\dot{\epsilon}_{II}^*}$$

$$\frac{\partial \eta^*}{\partial \dot{\epsilon}_{II}} = -\frac{1}{2} \frac{\eta^*}{\dot{\epsilon}_{II}^*} \quad (\text{Plastic case})$$

Strain rate derivatives

$$\dot{\epsilon}_{xx}(i,j) = \frac{v_x(i+1,j) - v_x(i,j)}{\Delta x} \quad \frac{\partial \dot{\epsilon}_{yy}(i,j)}{\partial v_y(i,j)} = -\frac{1}{\Delta y} \quad \frac{\partial \dot{\epsilon}_{yy}(i,j)}{\partial v_y(i,j+1)} = \frac{1}{\Delta y}$$

Second invariant contribution derivatives

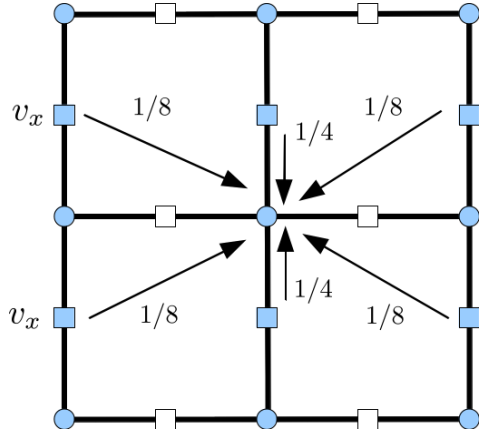
$$\Delta \dot{\epsilon}_{J2cen}(i,j) = \frac{1}{2} \left( \dot{\epsilon}_{xx}^2(i,j) + \dot{\epsilon}_{yy}^2(i,j) \right)$$

$$\frac{\partial \Delta \dot{\epsilon}_{J2cen}(i,j)}{\partial v_x(i,j)} = -\frac{1}{\Delta x} \dot{\epsilon}_{xx}(i,j) \quad \frac{\partial \Delta \dot{\epsilon}_{J2cen}(i,j)}{\partial v_x(i+1,j)} = \frac{1}{\Delta x} \dot{\epsilon}_{xx}(i,j)$$

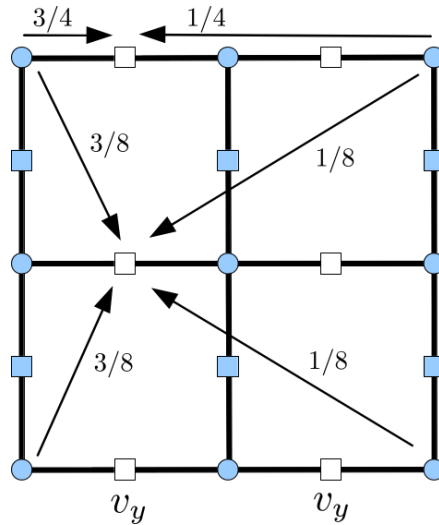
$$\frac{\partial \Delta \dot{\epsilon}_{J2cen}(i,j)}{\partial v_y(i,j)} = -\frac{1}{\Delta y} \dot{\epsilon}_{yy}(i,j) \quad \frac{\partial \Delta \dot{\epsilon}_{J2cen}(i,j)}{\partial v_y(i,j+1)} = \frac{1}{\Delta y} \dot{\epsilon}_{yy}(i,j)$$

# Galerkin Multigrid

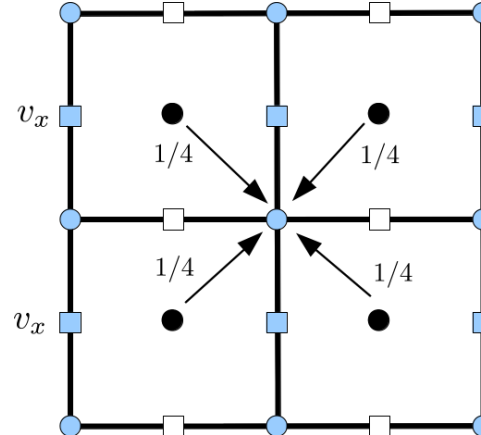
Velocity restriction



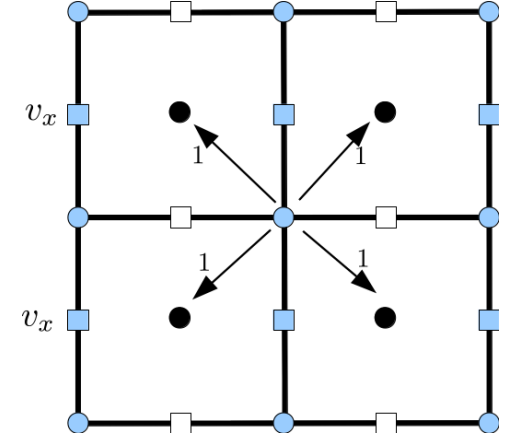
Velocity prolongation



Pressure restriction



Pressure prolongation



Described in Cai et al. 2014

## Galerkin coarsening

$$\mathbf{r}_{coarse} = \mathbf{R} \mathbf{r}_{fine} \quad \text{- Restriction}$$

$$\mathbf{x}_{fine} = \mathbf{P} \mathbf{x}_{coarse} \quad \text{- Prolongation}$$

$$\mathbf{A}_{coarse} = \mathbf{R} \mathbf{A}_{fine} \mathbf{P} \quad \text{- Coarsening}$$

## Preconditioners

$$\mathbf{P}_c = \begin{pmatrix} \mathbf{K} & \mathbf{G} \\ \mathbf{D} & -\frac{1}{\eta} \mathbf{I} \end{pmatrix}$$

(COUPLED)

Galerkin MG applied to full matrix

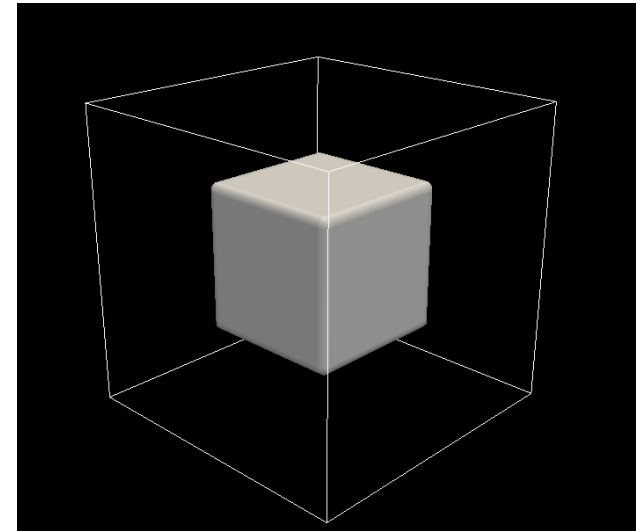
$$\mathbf{P}_u = \begin{pmatrix} \mathbf{K} & \mathbf{G} \\ & -\frac{1}{\eta} \mathbf{I} \end{pmatrix}$$

(BLOCK MG - uncoupled)

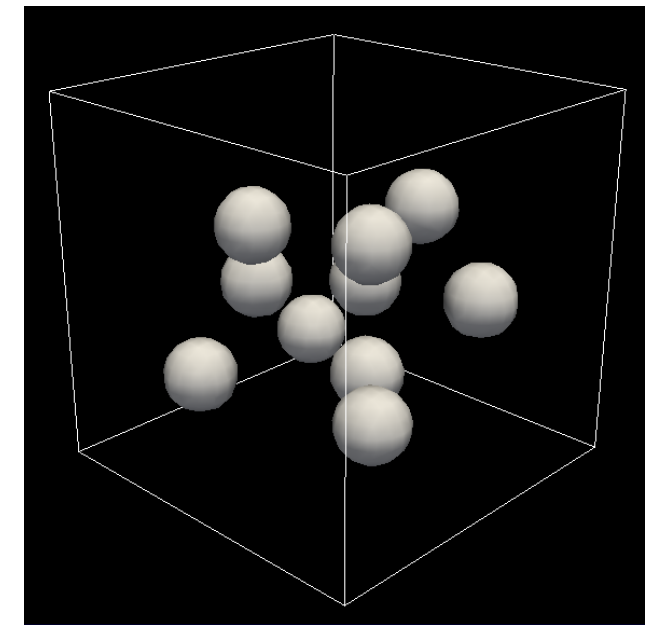
Galerkin MG applied to  $\mathbf{K}$  block only

# Coupled vs. Uncoupled MG (1 vs. 10 falling blocks)

64 <sup>3</sup> nodes 3 GMG levels <b>Viscosity contrast</b>	<b>Falling block setup</b>			
	<b>Coupled multigrid</b>		<b>Block MG</b>	
	# outer KSP it	Time [s]	# outer KSP it	Time [s]
1	7	6.1	9	6.4
10	10	8.2	13	8.4
100	12	9.6	20	11.9
1000	17	13.2	30	17.1
10000	40	29	71	38
1.00E+05	155	107	267	137



64 <sup>3</sup> nodes 3 GMG levels <b>Viscosity contrast</b>	<b>Multiple spheres setup</b>			
	<b>Coupled multigrid</b>		<b>Block MG</b>	
	# outer KSP it	Time [s]	# outer KSP it	Total solve [s]
1	7	6.1	6	3.9
10	10	8	11	6
100	15	11.7	18	10.2
1000	36	27.6	45	23
10000	114	82	154	80.5
1.00E+05	378	266	585	297



Viscosity sinker=1, viscosity matrix= 1/VC

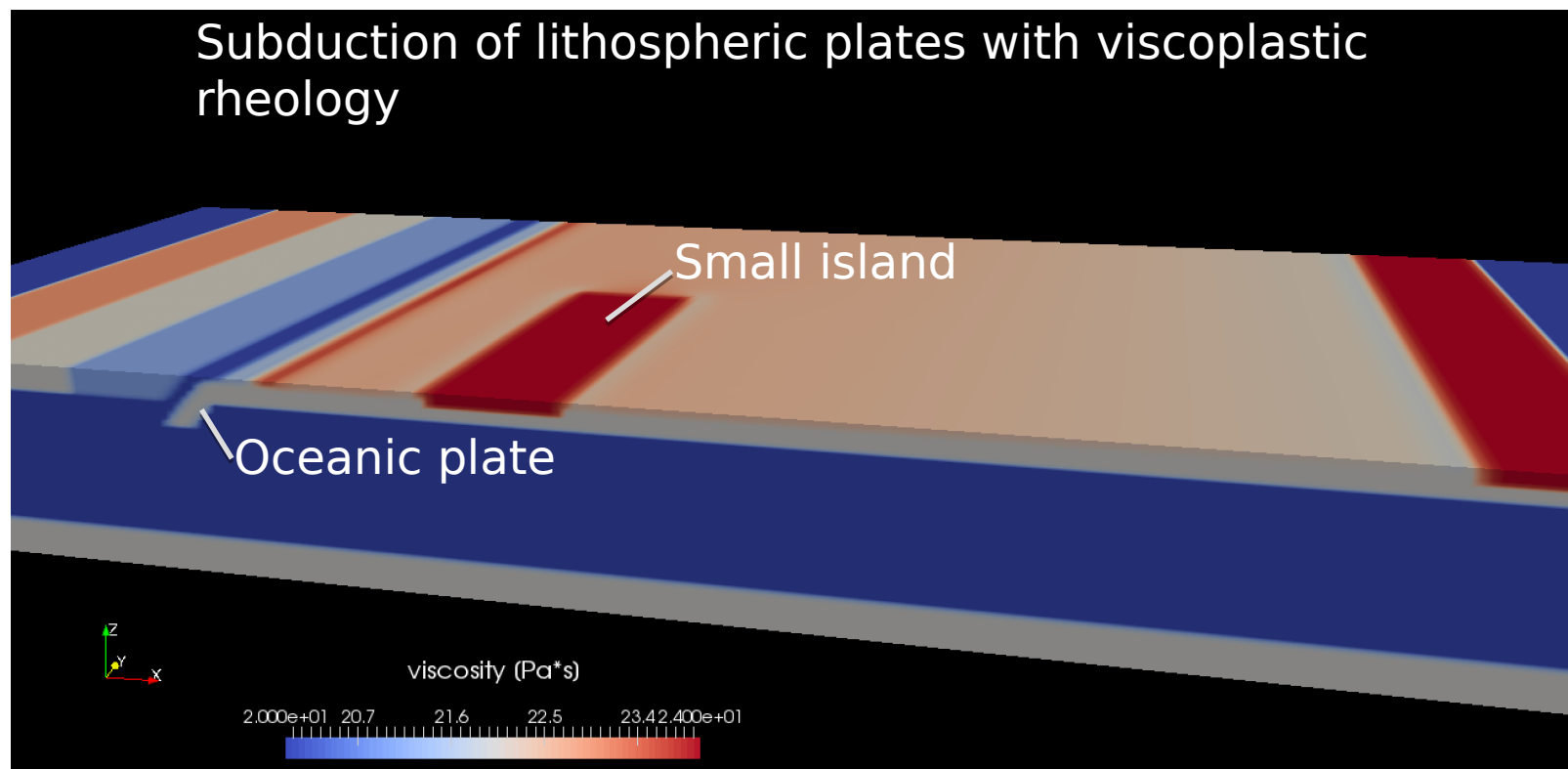
Multiple spheres is a more tricky problem  
Coupled/uncoupled have similar speeds

**Coupled:** 3 GMG levels with FGMRES (rtol 1e-6), Jacobi(20,20) as smoother; direct coarse grid, 4 cores

**Block:** FGMRES (rtol 1e-6) for full system with 1 V-cycle for the K-block, 3 GMG levels with Jacobi(20,20) as smoother and direct coarse grid



# Coupled vs. Uncoupled MG (typical production run)



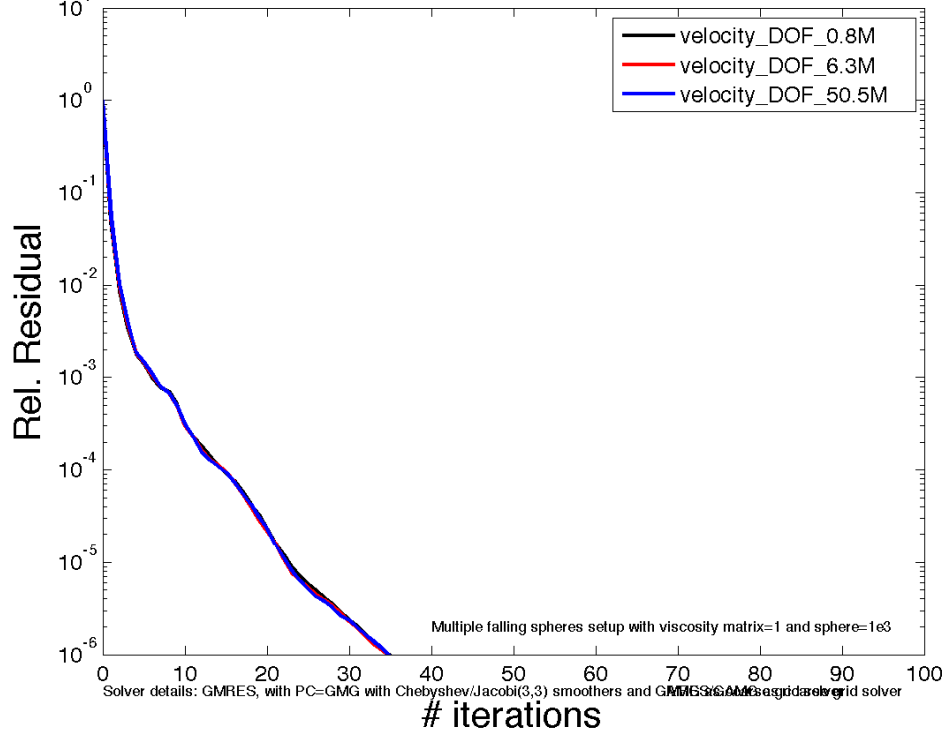
3 GMG levels	128x32x32		
Resolution	# SNES (nonlinear)	# KSP it (total)	Time per timestep [s]
Coupled MG	2	40	12
Block MG	2	100	24

4 GMG levels	256x64x64		
Resolution	# SNES (nonlinear)	# KSP it	Time [s]
Coupled MG	2	30	145
Block MG	5	250	759

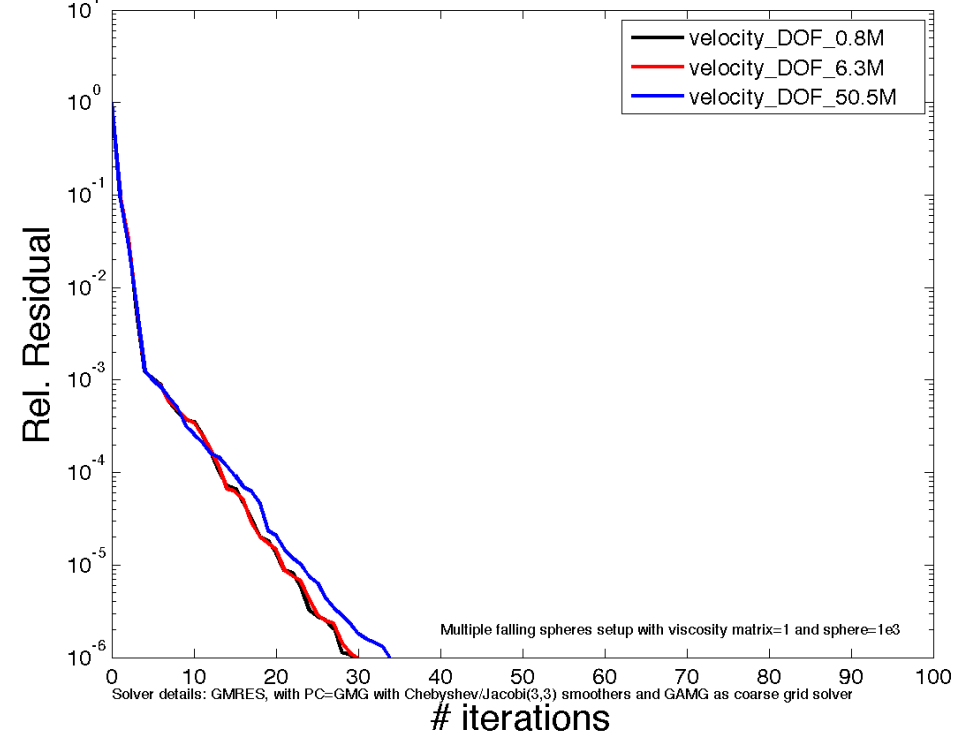
Coupled MG is significantly faster for this setup

# Weak scaling

Scalability of solving IK VP; PV 0l lu; pl=lf; gl (coupled MG)



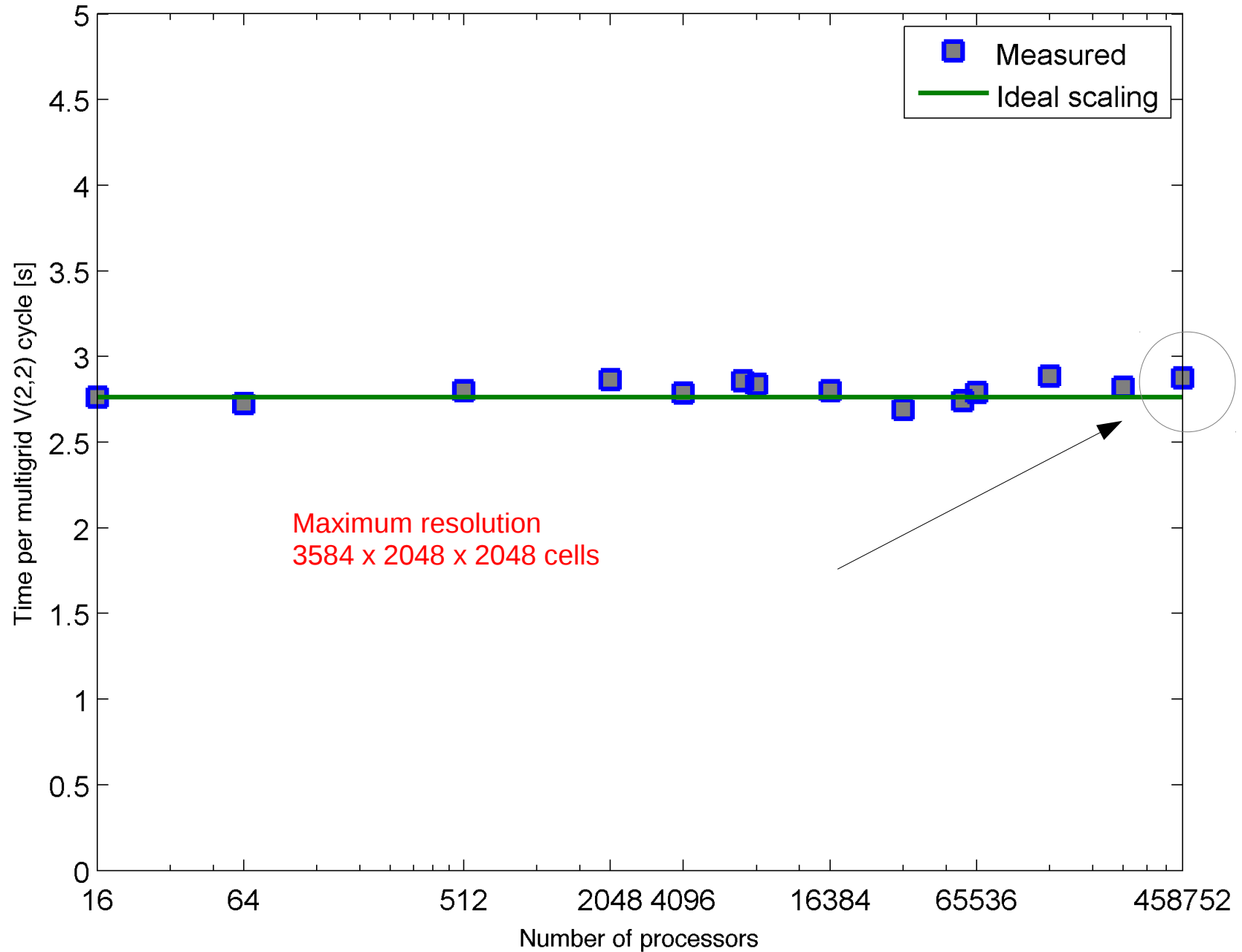
Scalability of solving Ku=f (velocity block)



Cores	Total grid size	MG Levels	Coarse Grid size	Velocity DOF	# KSP iterations	Time step [s]	Time/iterations [s]
64	128x128x128	2	64x64x64	6.3 Mio	65	155	2.38
512	256x256x256	3	64x64x64	50.5 Mio	67	159	2.37
4096	512x512x512	4	64x64x64	403 Mio	71	168	2.37
32768	1024x1024x1024	5	64x64x64	3.2 Bio	71	209	2.94
65536	2048x1024x1024	5	128x64x64	6.4 Bio	121	353	2.92
131072	2048x2048x1024	5	128x128x64	12.9 Bio	112	436	3.89
262144	2048x2048x2048	5	128x128x128	25.8 Bio	81	482	5.95

# Weak scaling

Weak scalability of LaMEM on JUQUEEN with  $32^3/\text{Core}$



# Continuum stress rates

Truesdell, Green-Naghdi and Jaumann rates:

$$\overset{\circ}{\sigma}{}^{TR} = \dot{\sigma} - l\sigma - \sigma l^T + \text{tr}[l]\sigma$$

$$\overset{\circ}{\sigma}{}^{GN} = \dot{\sigma} + \sigma\Omega - \Omega\sigma$$

$$\overset{\circ}{\sigma}{}^J = \dot{\sigma} + \sigma w - w\sigma$$

Spatial velocity gradient, spin and angular velocity tensors:

$$l = \dot{F}F^{-1}, \quad w = \frac{1}{2} \left( l - l^T \right), \quad \Omega = \dot{R}R^T$$

Deformation gradient:

$$F = \frac{\partial x}{\partial X}$$

Rotation and stretch tensors (polar decomposition)

$$F = RU$$

# Time integrated Jaumann stress rate (2D)

Jaumann rate expresses the rotated stress from previous time step as:

$$\tau_{ij}^* = \tau_{ij}^n + \Delta t (w_{ik}\tau_{kj}^n - \tau_{ik}^n w_{kj})$$

which can be viewed (e.g. Beuchert and Podladchikov, 2010) as a truncated Taylor series expansion of a simple stress rotation formula:

$$\tau_{ij}^* = R_{ik}\tau_{kl}^n R_{jl}$$

Jaumann rate expression imposes severe time step restrictions.

It is common (e.g. Gerya, 2010) to use the original stress rotation formula and estimate rotation angle from the time integration of the vorticity field:

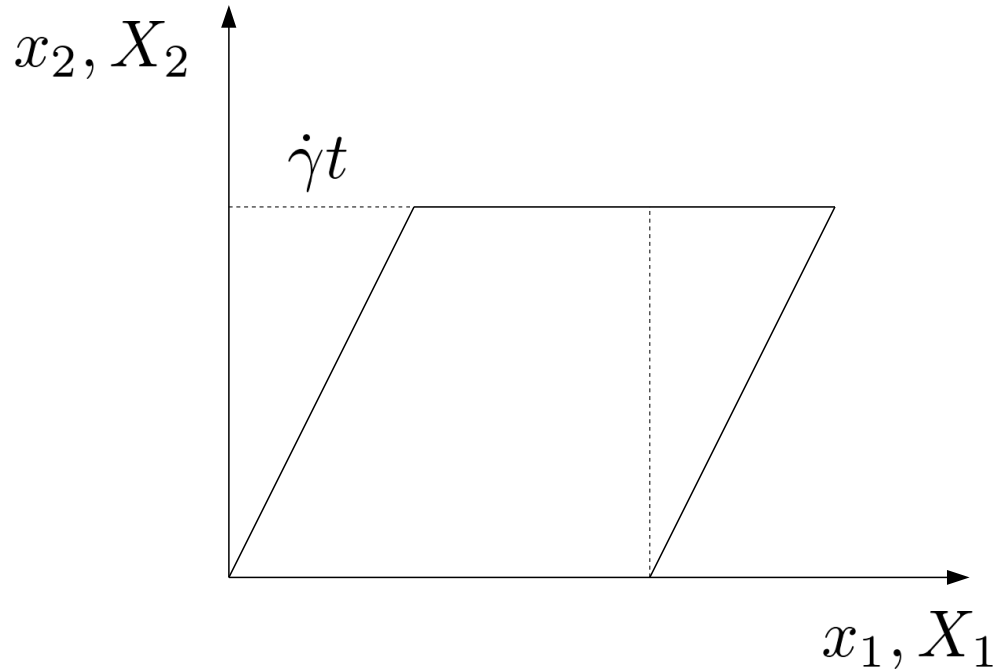
$$\theta = \frac{1}{2} \left( \frac{\partial v_y}{\partial x} - \frac{\partial v_x}{\partial y} \right) \Delta t$$

$$R = \begin{pmatrix} \cos \theta & -\sin \theta \\ \sin \theta & \cos \theta \end{pmatrix}$$

Beuchert and Podladchikov (2010). Viscoelastic mantle convection and lithospheric stresses. *Geophys. J. Int.*, 183, 35–63.

Gerya (2010) Introduction to numerical Geodynamic Modelling.

# Simple shear test



Material motion:

$$x_1 = X_1 + \dot{\gamma}t X_2$$

$$x_2 = X_2$$

Deformation gradient:

$$\mathbf{F} = \frac{\partial \mathbf{x}}{\partial \mathbf{X}} = \begin{pmatrix} 1 & \dot{\gamma}t \\ 0 & 1 \end{pmatrix}$$

Spatial velocity gradient, rate of deformation, and spin tensors:

$$\mathbf{l} = \dot{\mathbf{F}}\mathbf{F}^{-1} = \begin{pmatrix} 0 & \dot{\gamma} \\ 0 & 0 \end{pmatrix}, \quad \mathbf{d} = \begin{pmatrix} 0 & \frac{\dot{\gamma}}{2} \\ \frac{\dot{\gamma}}{2} & 0 \end{pmatrix}, \quad \mathbf{w} = \begin{pmatrix} 0 & \frac{\dot{\gamma}}{2} \\ -\frac{\dot{\gamma}}{2} & 0 \end{pmatrix}$$

Rotation tensor (polar decomposition) and angular velocity tensor:

$$\mathbf{R} = \begin{pmatrix} \cos \beta & \sin \beta \\ -\sin \beta & \cos \beta \end{pmatrix}, \quad \tan \beta = \frac{\dot{\gamma}t}{2}, \quad \mathbf{\Omega} = \dot{\mathbf{R}}\mathbf{R}^T = \left[ 1 + \left( \frac{\dot{\gamma}t}{2} \right)^2 \right]^{-1} \mathbf{w}$$



# Elastic case

Neo-Hookean (elastic stored energy function):

$$W = \frac{G}{2} (\bar{I}_1 - 3) + \frac{K}{2} (J - 1)^2$$

Determinant of deformation gradient (volume change):

$$J = \det [\mathbf{F}]$$

Volume-preserving left Cauchy-Green deformation tensor & first invariant:

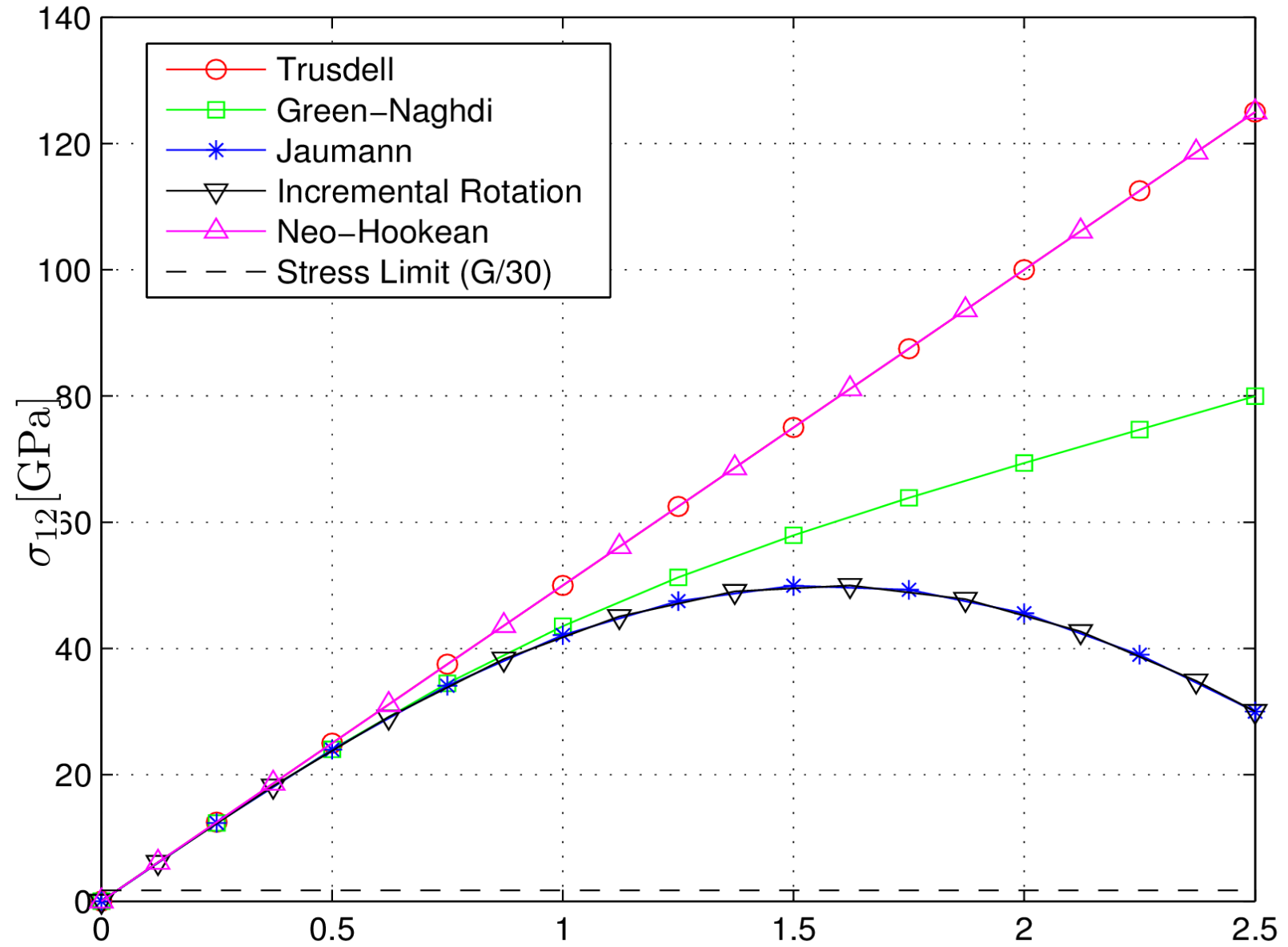
$$\bar{\mathbf{b}} = J^{-2/3} \mathbf{F} \mathbf{F}^T, \quad \bar{I}_1 = \text{tr} [\bar{\mathbf{b}}]$$

Cauchy stress:

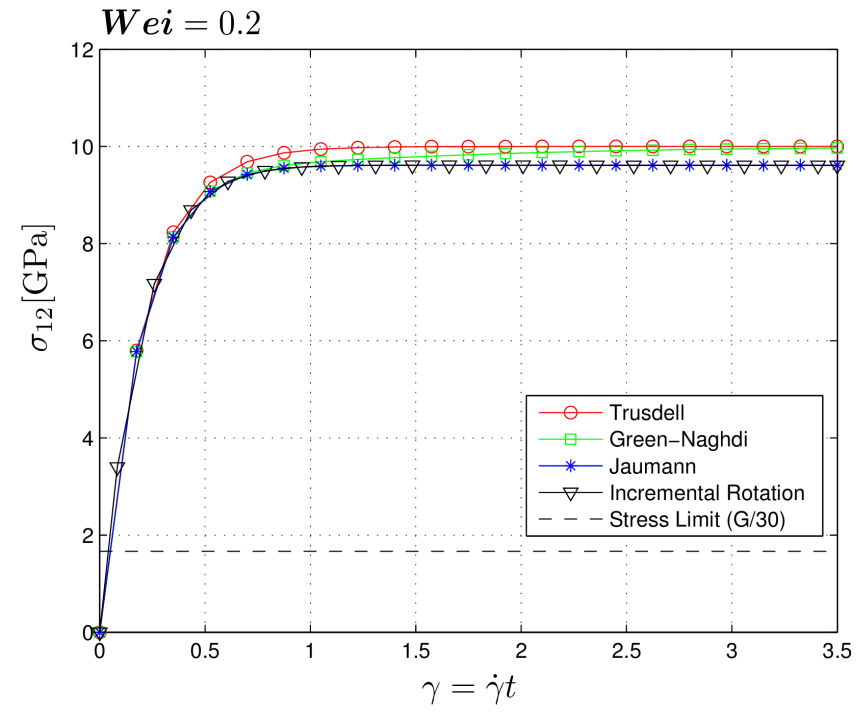
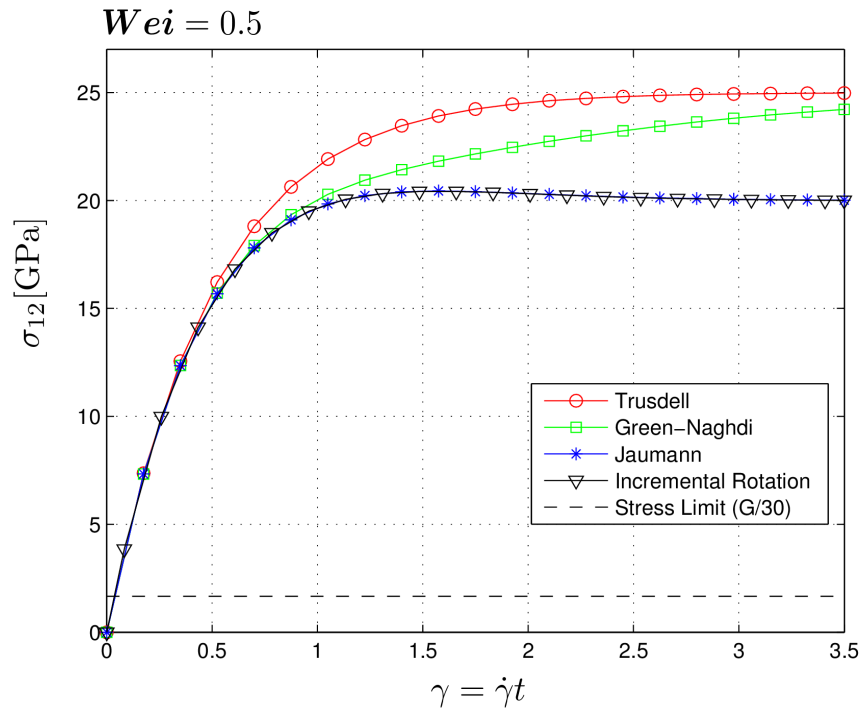
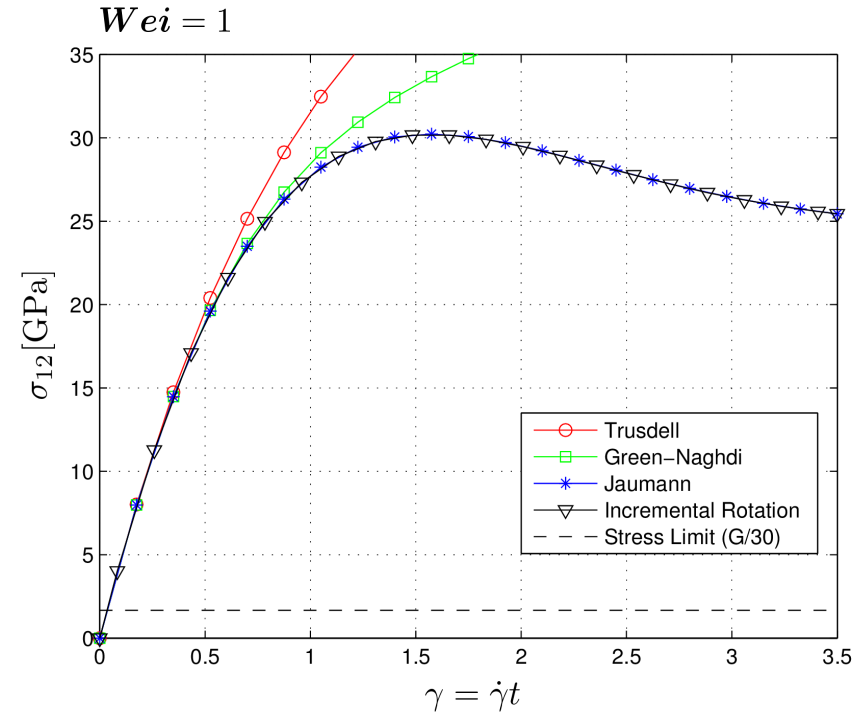
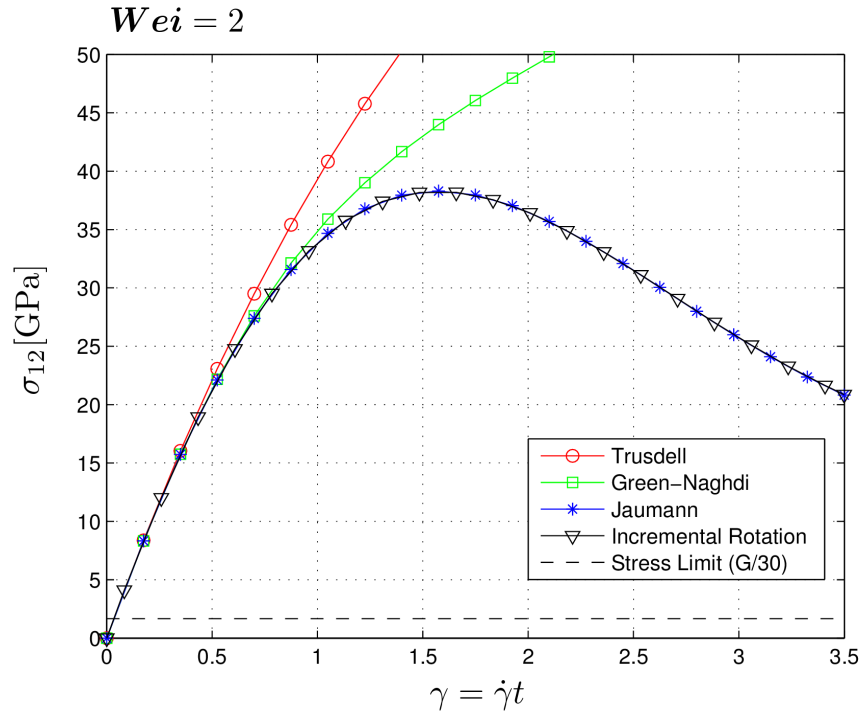
$$\boldsymbol{\sigma} = J^{-1} \mathbf{F} \frac{\partial W}{\partial \mathbf{F}} = J^{-1} G \text{dev} [\bar{\mathbf{b}}] + K(J - 1) \mathbf{1}$$

$$\boldsymbol{\sigma} = G \text{dev} [\mathbf{b}] = G \begin{pmatrix} \frac{2}{3}(\dot{\gamma}t)^2 & \dot{\gamma}t & 0 \\ \dot{\gamma}t & -\frac{1}{3}(\dot{\gamma}t)^2 & 0 \\ 0 & 0 & -\frac{1}{3}(\dot{\gamma}t)^2 \end{pmatrix}$$

# Elastic case



# Visco-Elastic case (Weissenberg number)

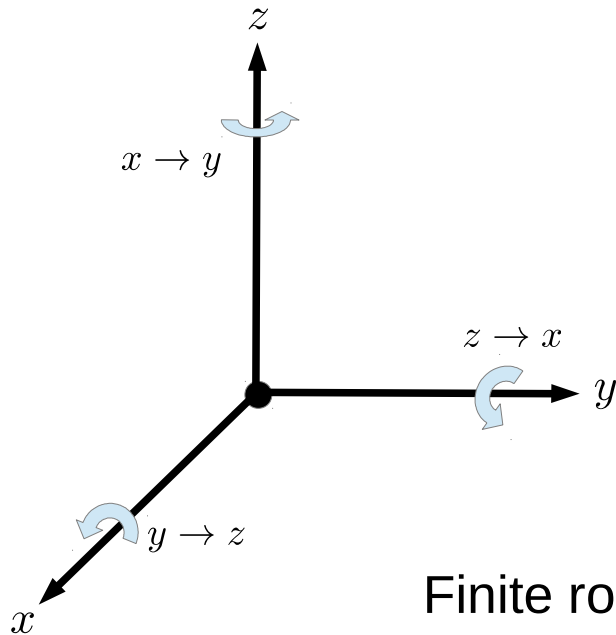


# 3D generalization of 2D incremental rotation rate

Can we use a similar method in 3D?

In 2D vorticity pseudo-vector has a single component and instantaneous rotation axis is always perpendicular to the plane.

In 3D vorticity pseudo-vector has three components and instantaneous rotation axis can change in time:



$$\begin{pmatrix} w_x \\ w_y \\ w_z \end{pmatrix} = \begin{pmatrix} \frac{\partial v_z}{\partial y} - \frac{\partial v_y}{\partial z} \\ \frac{\partial v_x}{\partial z} - \frac{\partial v_z}{\partial x} \\ \frac{\partial v_y}{\partial x} - \frac{\partial v_x}{\partial y} \end{pmatrix}$$

Positive rotation directions: Counter-clockwise  
Coordinate system: Right-handed

Finite rotations around coordinate axis unfortunately do not commute in 3D. Nevertheless the 3D generalization of a 2D algorithm yields reasonable results (Rubinstein and Atluri, 1983).

# 3D generalization of 2D incremental rotation rate

The 3D algorithm can be summarized as follows:

[1] Compute vorticity vector magnitude:  $w = \sqrt{w_x^2 + w_y^2 + w_z^2}$

[2] Compute unit rotation axis: 
$$\begin{pmatrix} n_x \\ n_y \\ n_z \end{pmatrix} = w^{-1} \begin{pmatrix} w_x \\ w_y \\ w_z \end{pmatrix}$$

[3] Integrate incremental rotation angle:  
*(average angular velocity is two times smaller than the vorticity vector magnitude)* 
$$\theta = \Delta t \left( \frac{w}{2} \right)$$

[4] Evaluate rotation matrix using Euler-Rodrigues formula:

$$R = \cos \theta \begin{pmatrix} 1 & & \\ & 1 & \\ & & 1 \end{pmatrix} + \sin \theta \begin{pmatrix} 0 & -n_z & n_y \\ n_z & 0 & -n_x \\ -n_y & n_x & 0 \end{pmatrix} + (1 - \cos \theta) \begin{pmatrix} n_x^2 & n_x n_y & n_x n_z \\ n_y n_x & n_y^2 & n_y n_z \\ n_z n_x & n_z n_y & n_z^2 \end{pmatrix}$$

[5] Rotate stress:  $\tau^* = R \tau^n R^T$

# Comparison with Jaumann stress rate

Consider a rather extreme case of 3D accelerated periodic rotational motion:

$$v_x = r \cos \theta \dot{\theta} \cos \phi - r \sin \theta \sin \phi \dot{\phi}$$

$$v_y = r \cos \theta \dot{\theta} \sin \phi + r \sin \theta \sin \phi \dot{\phi}$$

$$v_z = -r \sin \theta \dot{\theta}$$

$$\phi(t) = 2\pi t^5$$

$$\theta(t) = \frac{\pi}{2} + \frac{\pi}{8} \sin(4\pi t^5)$$

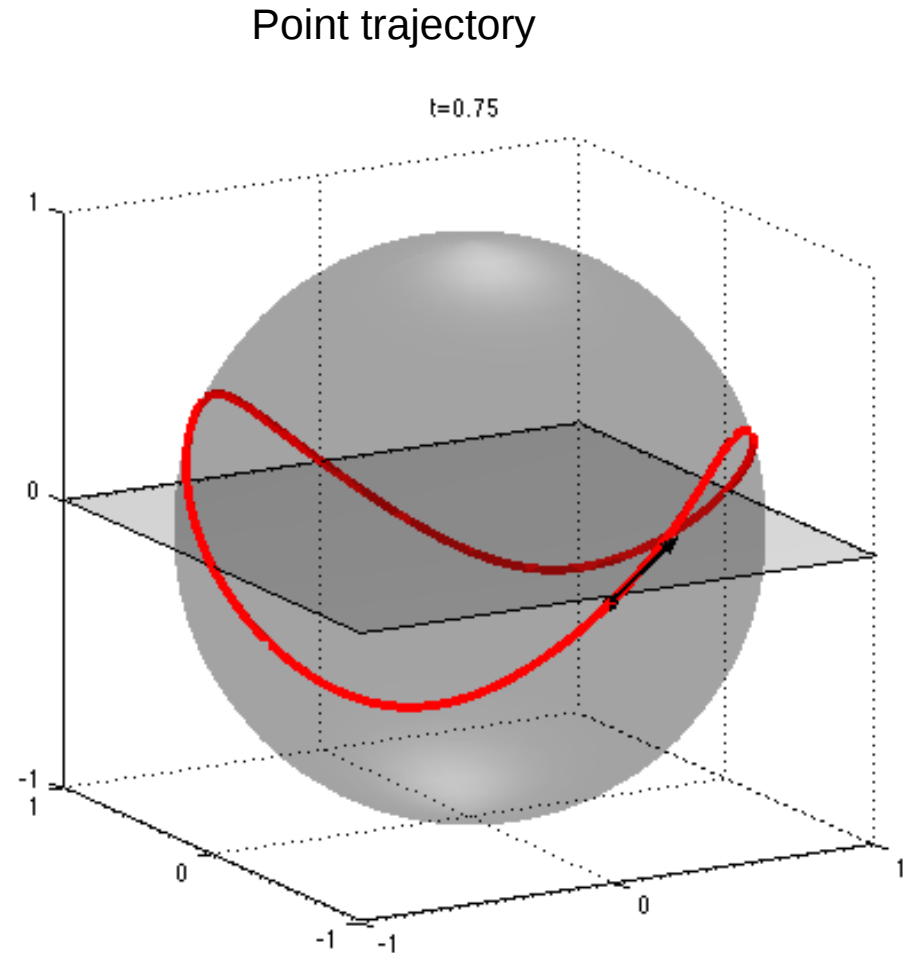
Assign randomly the stress tensor components at the initial time and integrate by three different methods:

[A] Jaumann forward Euler

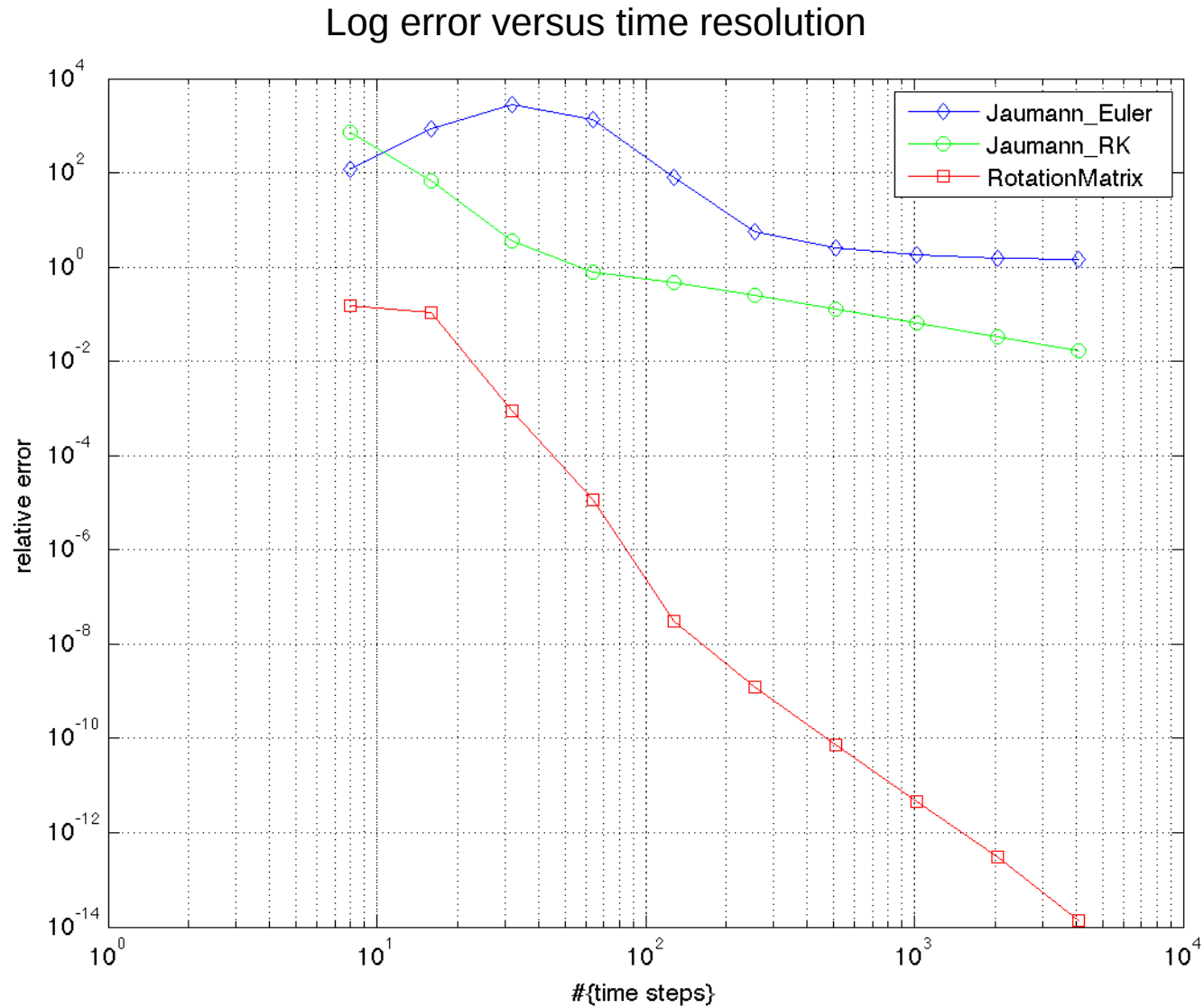
[B] Jaumann 4-th order Runge-Kutta

[C] Generalized 3D rotation matrix

After a full turn the stress components should be the same as in the beginning.

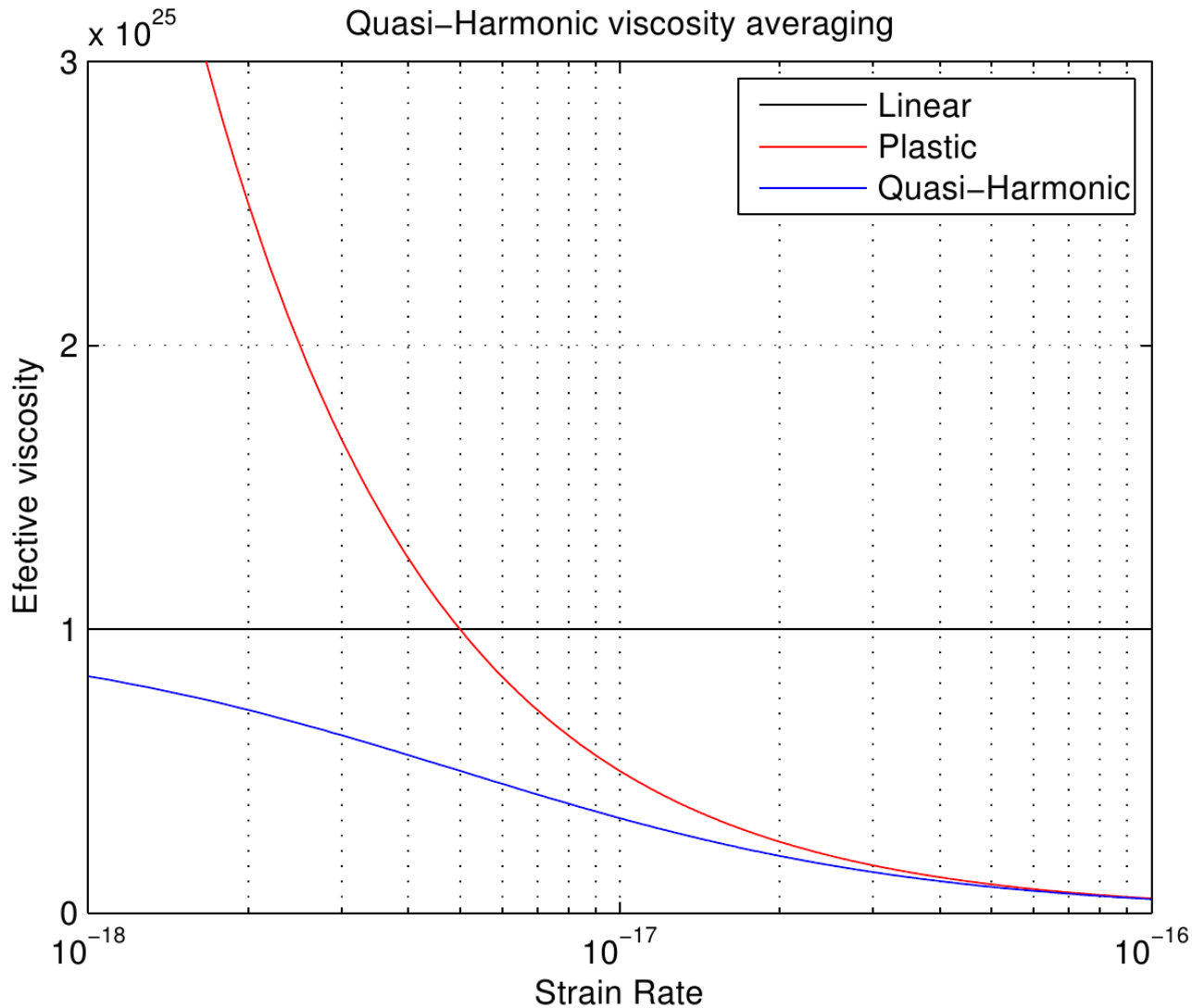


# Comparison with Jaumann stress rate



Conclusion: 3D rotation matrix yields much better results than Jaumann rate

# Minimum vs. quasi-harmonic plastic viscosity



Plastic viscosity:

$$\eta_p = \frac{\tau_Y}{2\dot{\epsilon}_{II}^*}$$

Minimum viscosity:

$$\eta^* = \min(\eta, \eta_p)$$

Quasi-harmonic viscosity:

$$\eta^* = \left( \frac{1}{\eta} + \frac{1}{\eta_p} \right)^{-1}$$

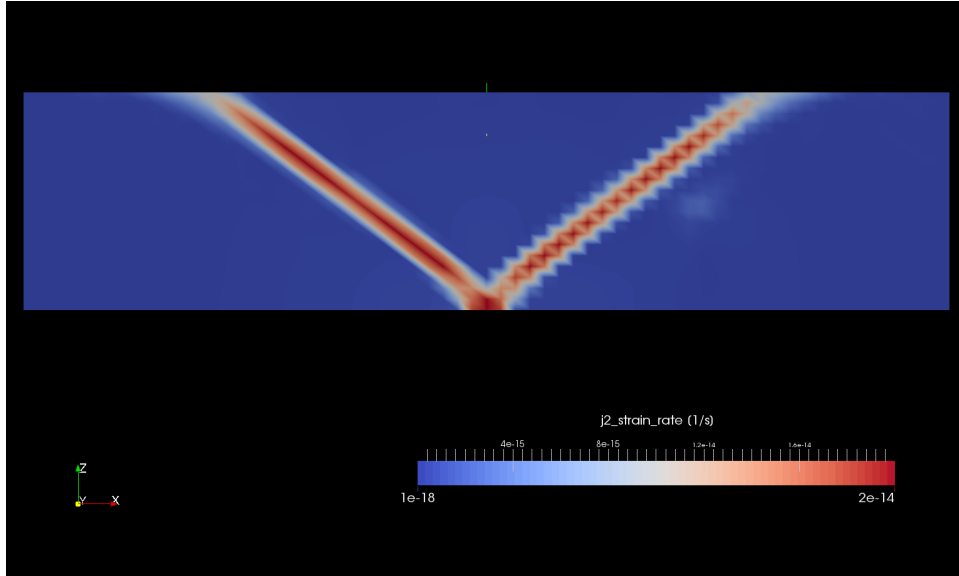
Both are coincident only at high strain rates

Quasi-harmonic has spurious plastic deformation below yield!

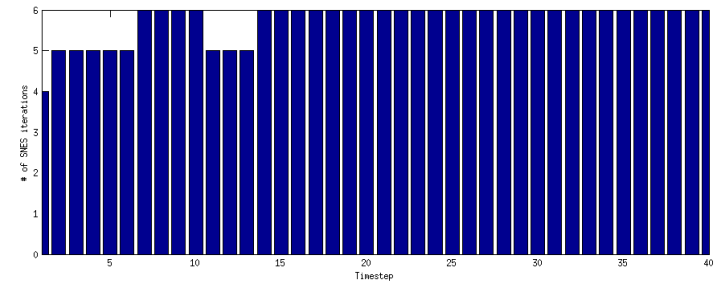
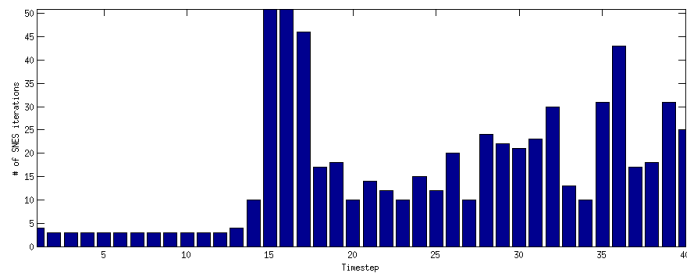
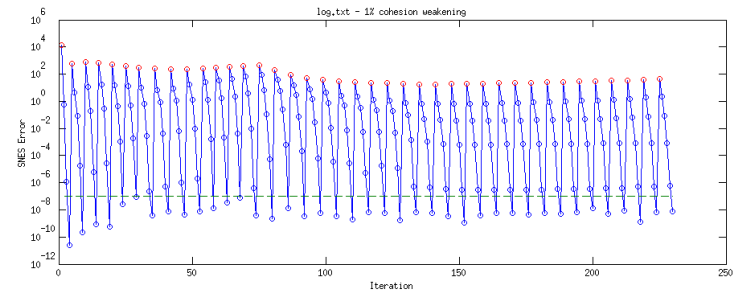
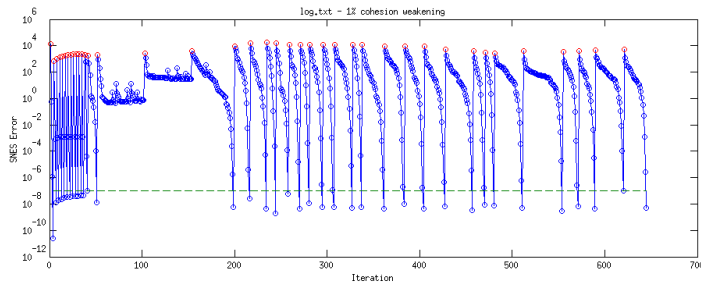
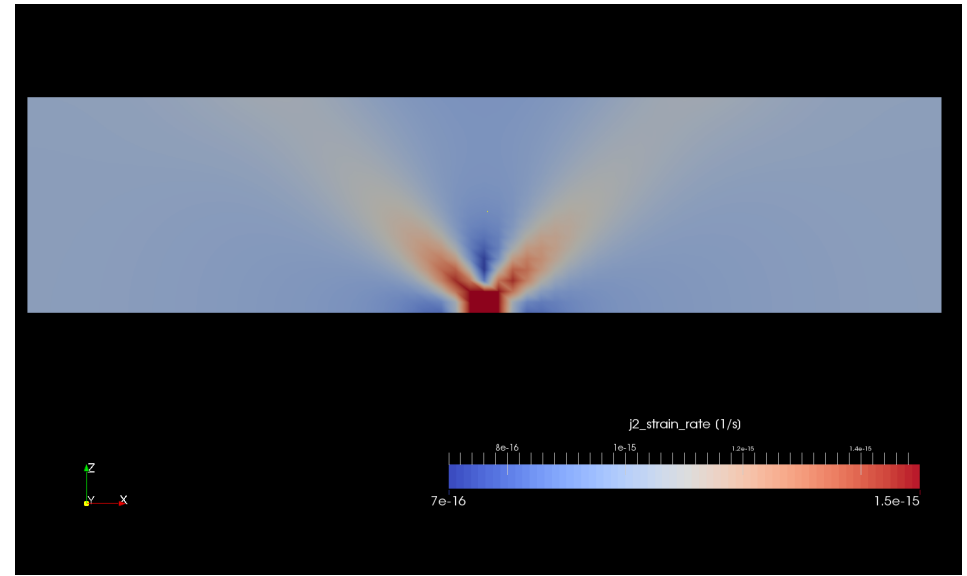


# Minimum vs. quasi-harmonic plastic viscosity

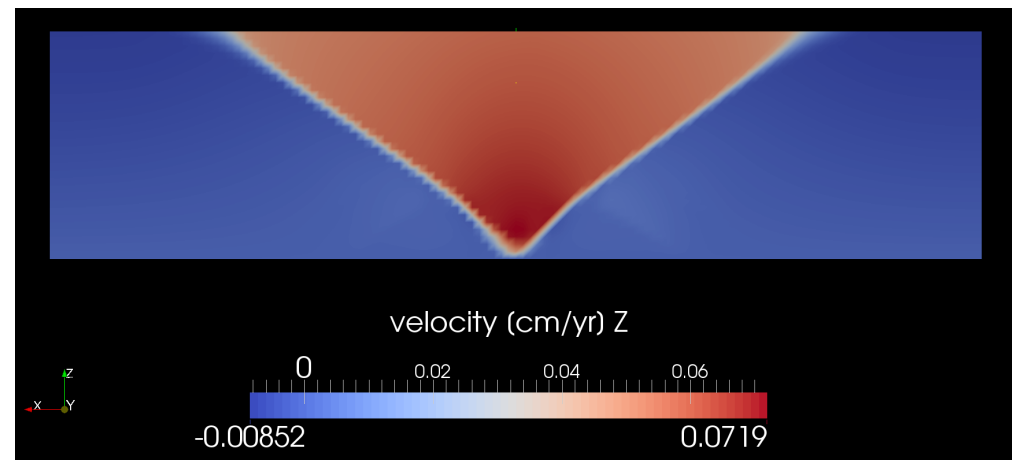
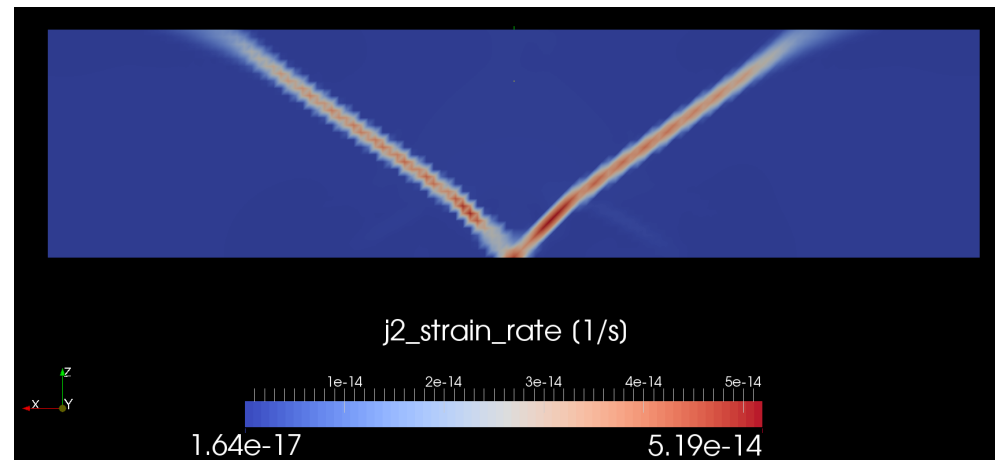
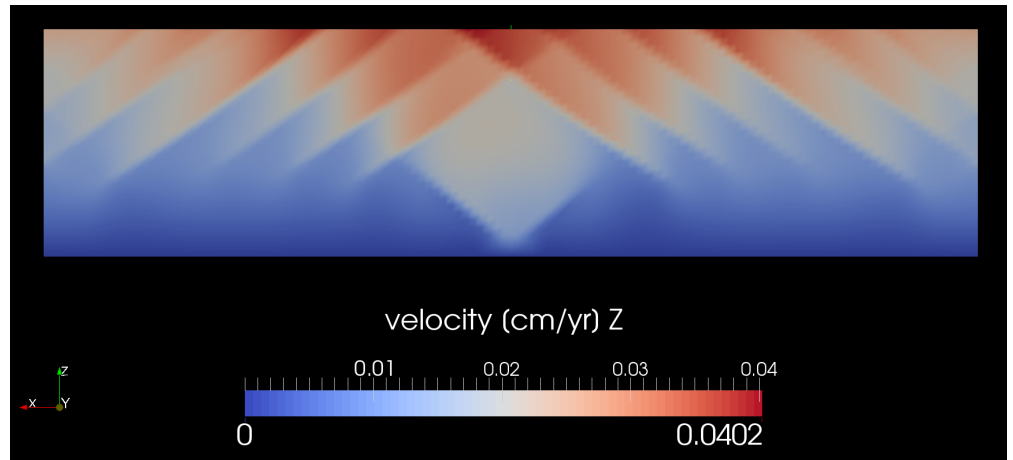
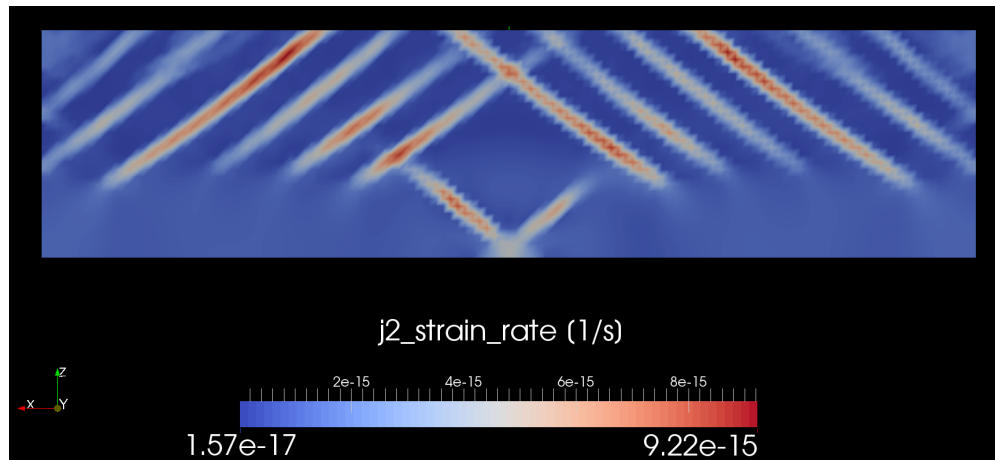
Minimum viscosity model  
Hard to converge, sharp localization



Quasi-harmonic viscosity model  
Easy to converge, very pure localization



# Plasticity convergence issues

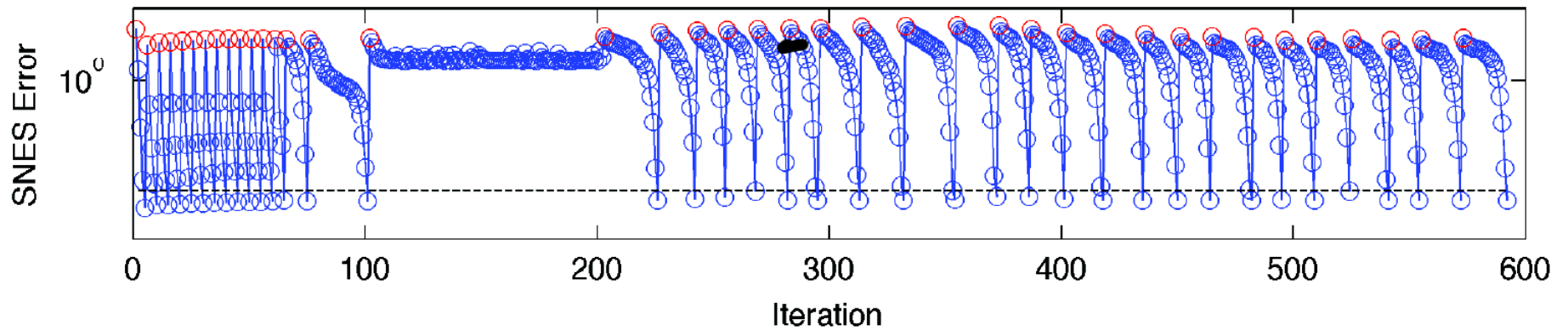


Plastic localization setup

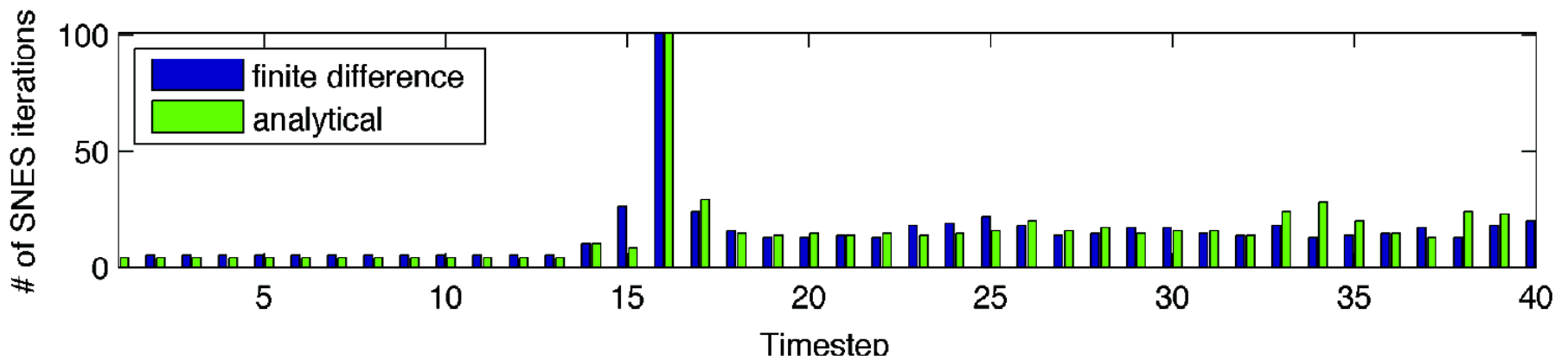
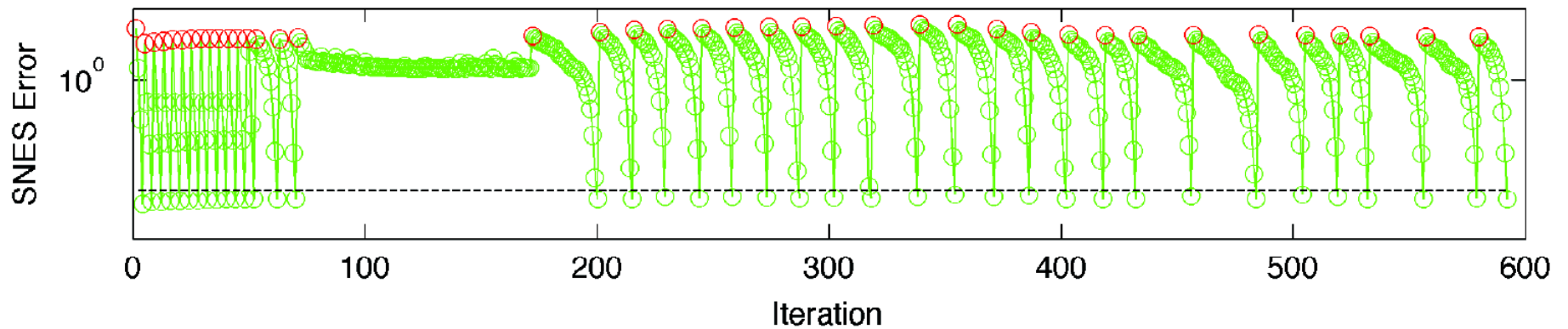
Drucker-Prager elasto-plastic rheology

# Plasticity convergence issues

EGU\_poster\_mffd\_128by32\_ew.dat - 50% C/ϕ Weakening between  $e_p = 10^{-9}$ - $10^{-3}$



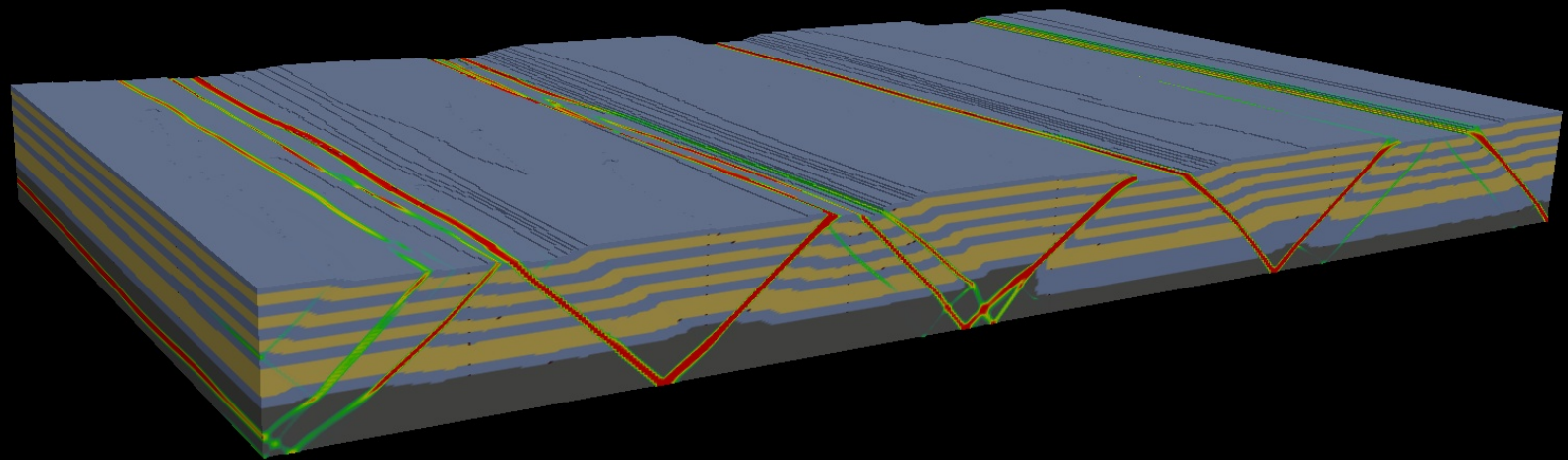
EGU\_poster\_analytical\_128by32\_ew.dat - 50% C/ϕ Weakening between  $e_p = 10^{-9}$ - $10^{-3}$



# Plasticity convergence issues (summary)

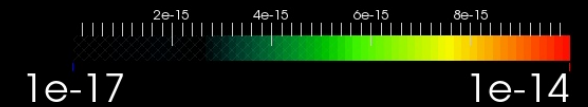
- Elasto-plastic setups converge better than visco-plastic
- Strain softening facilitates convergence
- Sometimes non-convergent solutions are reasonable (continuation is possible)
- A combination of Newton and Picard is necessary
- Line search and Eisenstat-Walker algorithms are helpful
- Visco-plastic pressure-dependent rheology may be not universally solvable (Spiegelman et al., 2016) despite quasi-harmonic averaging.
- Quasi-harmonic averaging produces pure localization, but fast to converge
- Analytical Jacobian doesn't help to accelerate convergence

# 3D Multilayer detachment folding (2D heterogeneity)



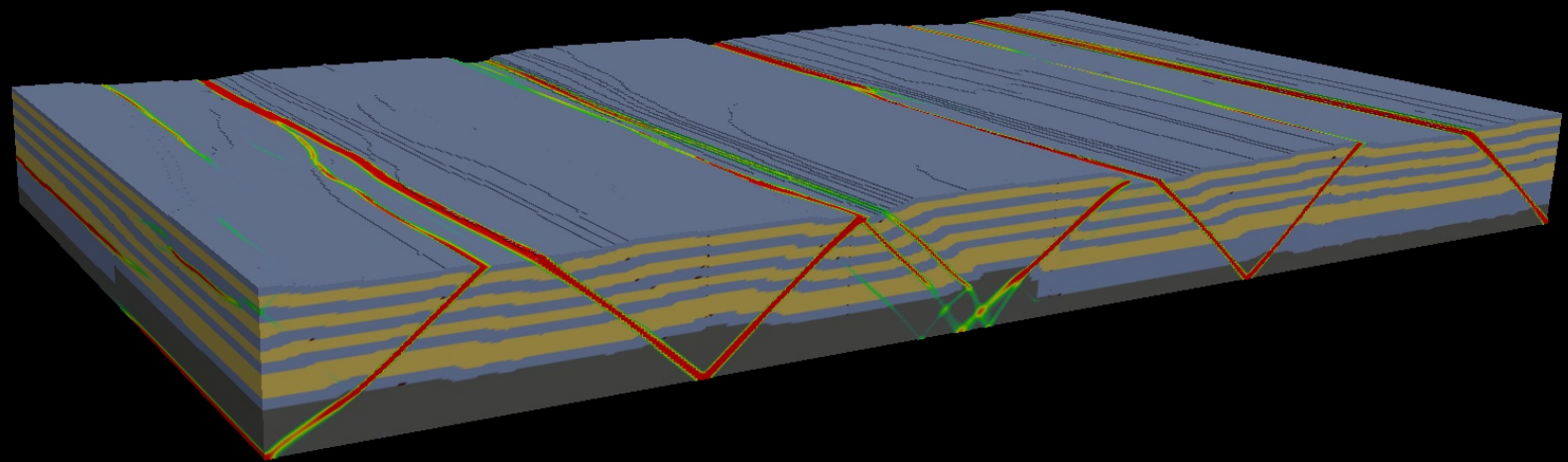
3.069 Myrs

strain rate (1/s)



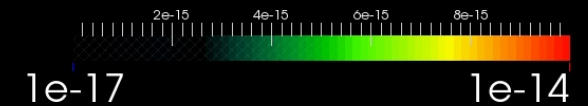
Grid resolution: 512 x 256 x 128 cells

# 3D Multilayer detachment folding (3D heterogeneity)



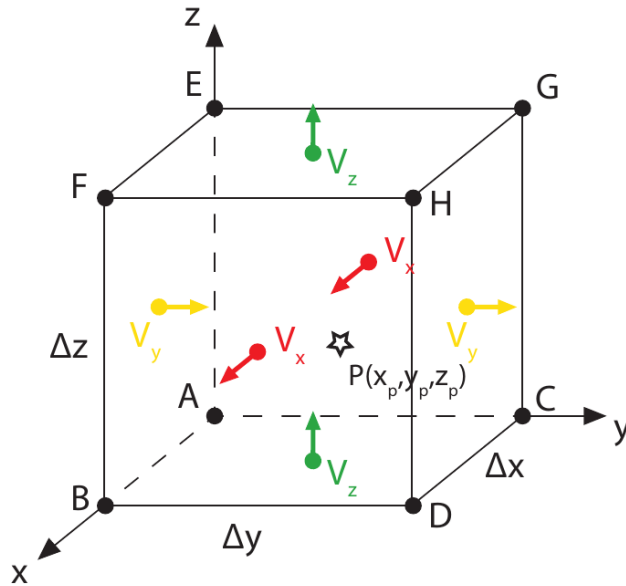
3.110 Myrs

strain rate (1/s)



Grid resolution: 512 x 256 x 128 cells

# Conservative velocity interpolation (CVI)



Wang et al. [2015]

Enough for FE

Not enough for FDSTAG

Velocities are not in the corners

Prevent unphysical marker dispersion:

$$V_i^P = V_i^L + \Delta V_i$$

Liner interpolation:

$$V_i^L(x_p, y_p, z_p) = (1-x_p) \times (1-y_p) \times [(1-z_p) \times V_i^A + z_p \times V_i^E] + \\ x_p \times (1-y_p) \times [(1-z_p) \times V_i^B + z_p \times V_i^F] + \\ (1-x_p) \times y_p \times [(1-z_p) \times V_i^C + z_p \times V_i^G] + \\ x_p \times y_p \times [(1-z_p) \times V_i^D + z_p \times V_i^H],$$

Correction:

$$\Delta V_x = x_p(1-x_p)(C_{10} + z_p C_{12})$$

$$\Delta V_y = y_p(1-y_p)(C_{30} + x_p C_{31})$$

$$\Delta V_z = z_p(1-z_p)(C_{20} + y_p C_{23})$$

$$C_{12} = \frac{\Delta x}{2\Delta y} [-V_y^A + V_y^B + V_y^C - V_y^D + V_y^E - V_y^F - V_y^G + V_y^H]$$

$$C_{23} = \frac{\Delta z}{2\Delta x} [-V_x^A + V_x^B + V_x^C - V_x^D + V_x^E - V_x^F - V_x^G + V_x^H]$$

$$C_{31} = \frac{\Delta y}{2\Delta z} [-V_z^A + V_z^B + V_z^C - V_z^D + V_z^E - V_z^F - V_z^G + V_z^H]$$

$$C_{10} = \frac{\Delta x}{2\Delta z} [V_z^A - V_z^B - V_z^E + V_z^F] + \frac{\Delta x}{2\Delta y} [V_y^A - V_y^B - V_y^C + V_y^D + C_{31}]$$

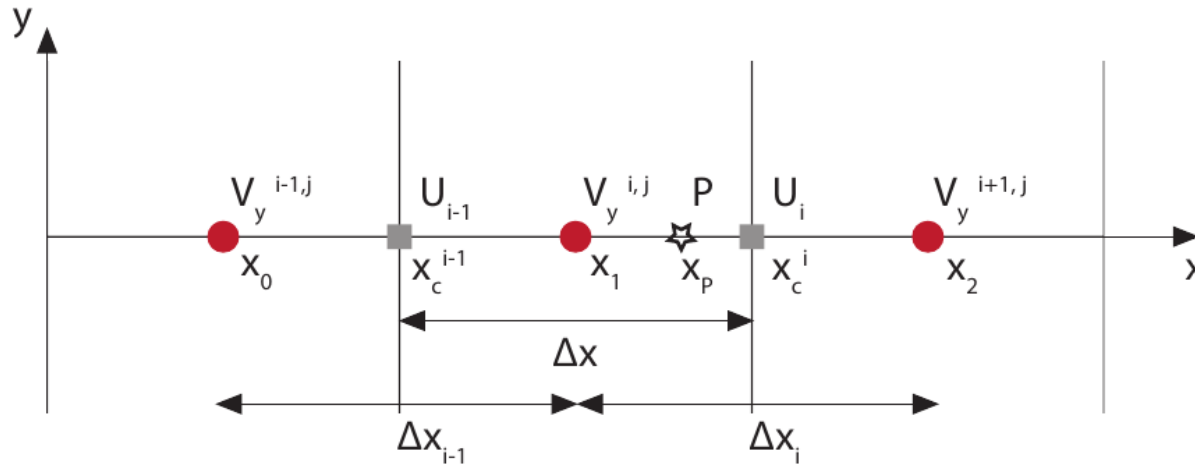
$$C_{20} = \frac{\Delta z}{2\Delta x} [V_x^A - V_x^B - V_x^E + V_x^F + C_{12}] + \frac{\Delta z}{2\Delta y} [V_y^A - V_y^C - V_y^E + V_y^G]$$

$$C_{30} = \frac{\Delta y}{2\Delta x} [V_x^A - V_x^B - V_x^C + V_x^D] + \frac{\Delta y}{2\Delta z} [V_z^A - V_z^C - V_z^E + V_z^G + C_{23}]$$

# Minmod Interpolant

Interpolate velocities from faces to corners:

- linear - Lin
- quadratic - Q2
- spline quadratic SQ2
- Minmod

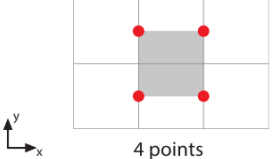
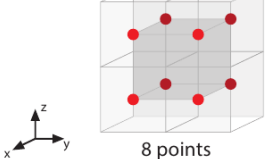
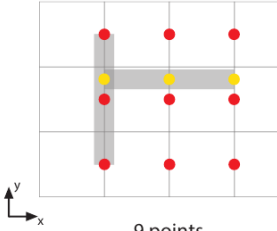
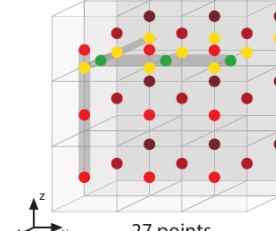
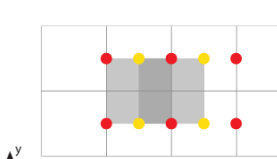
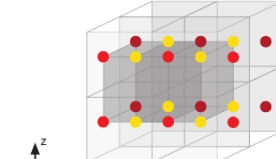
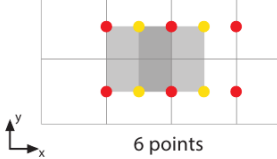
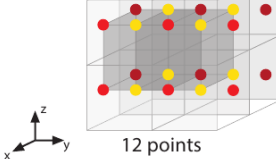


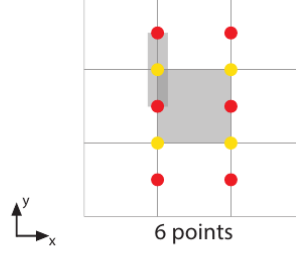
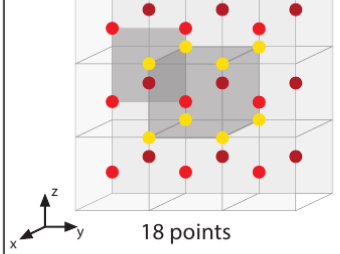
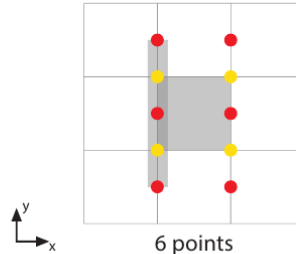
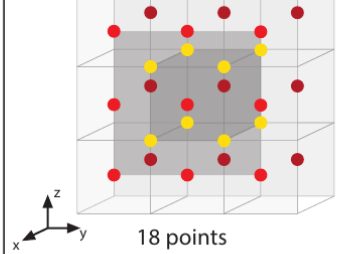
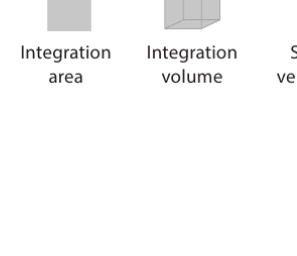
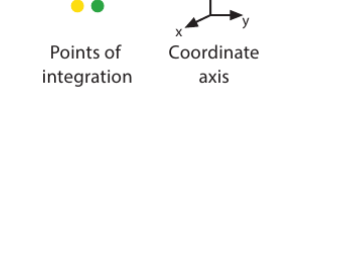
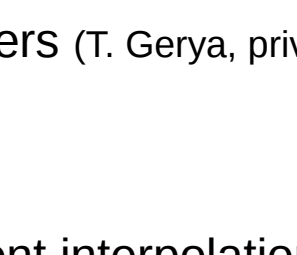
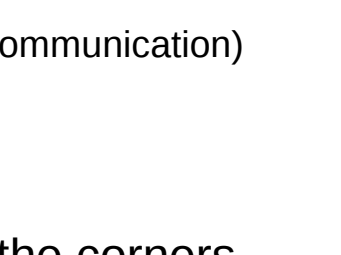



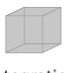



$$U_i = V_y^{i,j} - \frac{\Delta x}{2} \minmod \left( \frac{V_y^{i+1,j} - V_y^{i,j}}{\Delta x_i}, \frac{V_y^{i,j} - V_y^{i-1,j}}{\Delta x_{i-1}} \right)$$

$$\minmod(A, B) = \begin{cases} A, & \text{if } A \cdot B > 0 \text{ and } |A| \leq |B| \\ B, & \text{if } A \cdot B > 0 \text{ and } |A| > |B| \\ 0, & \text{if } A \cdot B \leq 0 \end{cases}$$



# Conservative velocity interpolation (CVI)

Interpolation stencils		2-D	3-D
Direct interpolation	Linear (Lin)	 4 points	 8 points
	Quadratic (L1Q2*, Q2)	 9 points	 27 points
	Spline Quadratic (L1SQ2*, SQ2)	 9 points	 27 points
	Empirical (LinP**)	 6 points	 12 points

Correction interpolation	Linear (CorrLin)	 6 points	 18 points
	Minmod limiter (CorrMinmod)	 6 points	 18 points
	Quadratic (CorrQ2)	 9 points	 27 points
	Spline Quadratic (CorrSQ2)	 9 points	 27 points
legend:  2D grid  3D grid  Integration area  Integration volume  Staggered velocity point  Points of integration  Coordinate axis			

Püsök et al. [2016] (Submitted)

Direct interpolation methods don't apply correction

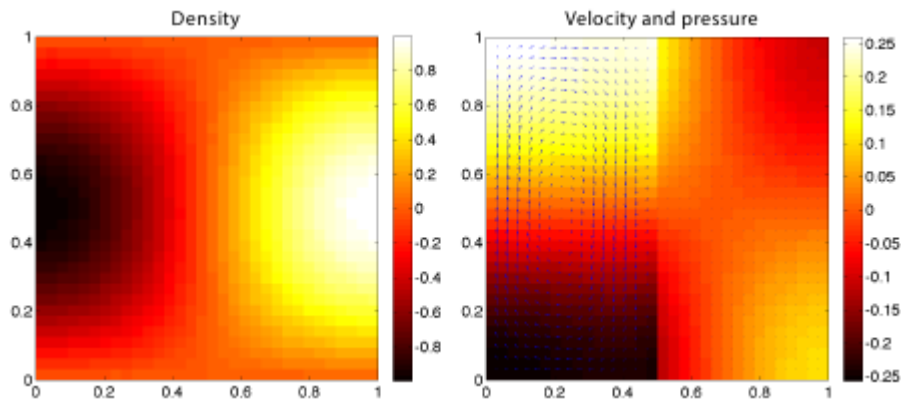
**LinP** interpolates from corners and pressure nodes cell centers (T. Gerya, private communication)

$$V_i^P = AV_i^{Lin} + (1 - A)V_i^{pressure}$$

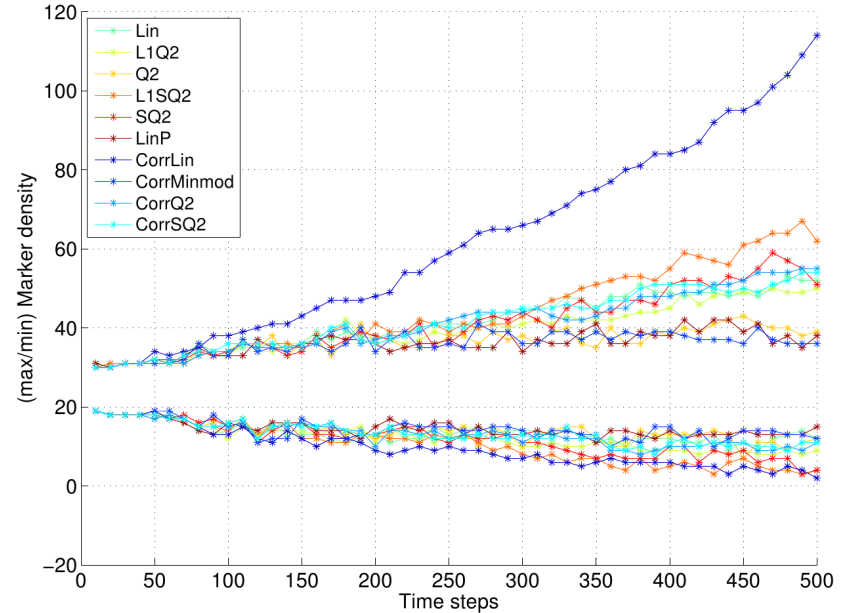
Corrected interpolation methods apply correction after different interpolation to the corners

# Velocity interpolation comparison

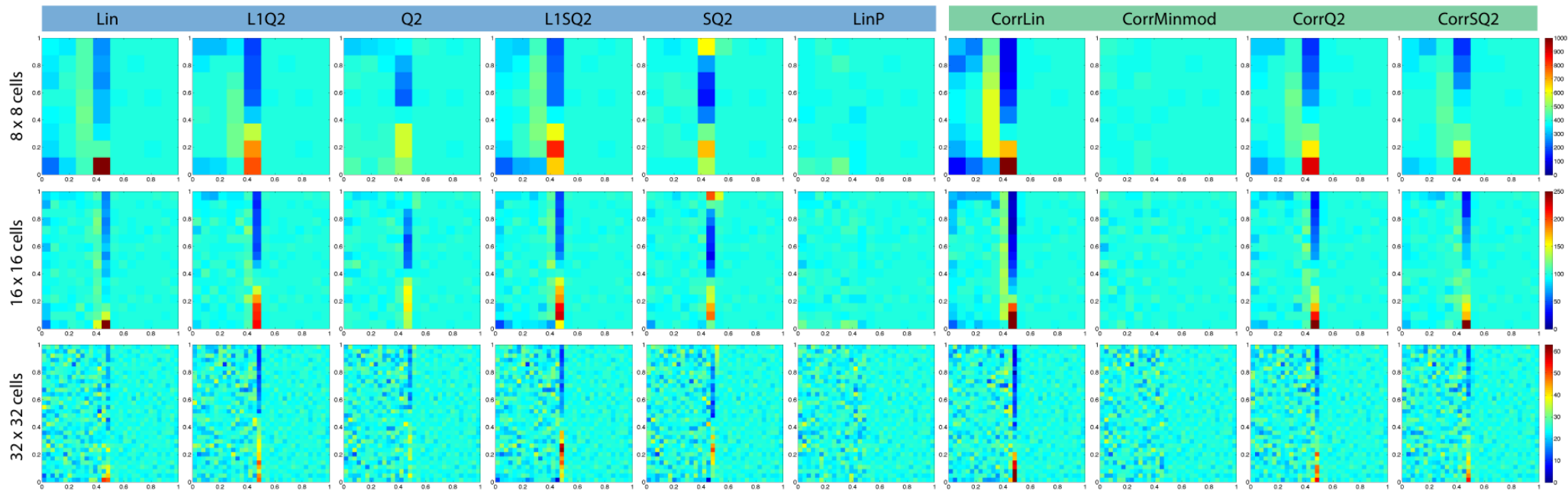
## SolCx benchmark



Advection: Runge-Kutta 4th order



## Marker density distribution



LinP (Gerya) and CorrMinmod produce best results.  
More details are coming soon Püsök et al. [2016]

# Gradient-based inversion methods

Minimize misfit function ( $F$ ), formulated in terms of model parameters ( $p$ )

$$\min_p (F(p))$$

Gradient descent:  $p_{n+1} = p_n - \gamma G(p_n)$

$$G = \frac{dF}{dp} \quad \text{- gradient vector}$$

Newton method:  $p_{n+1} = p_n - \alpha H(p_n)^{-1} G(p_n)$

$$H = \frac{dG}{dp} \quad \text{- Hessian matrix}$$

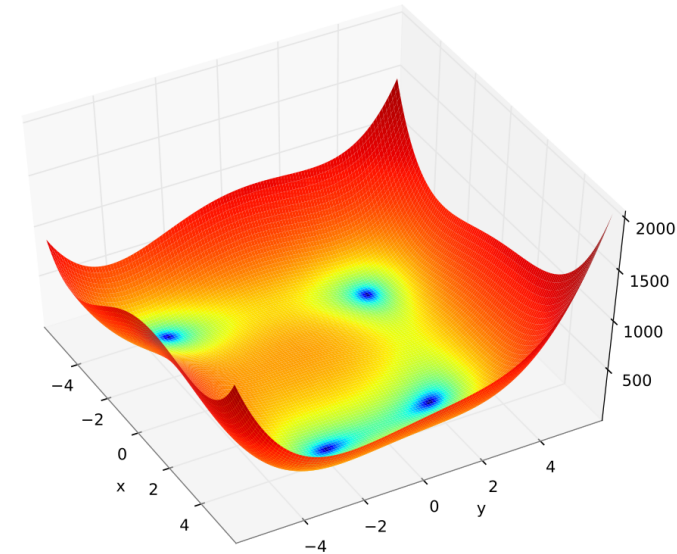
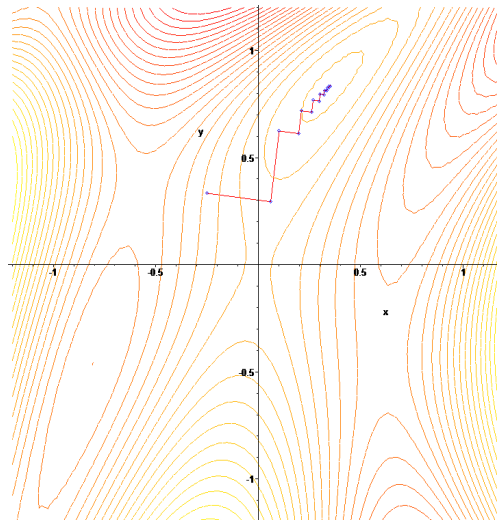
Hessian matrix can be efficiently approximated by BFGS algorithm

## DISADVANTAGES:

- *Requires derivatives*
- *Doesn't sample misfit function*
- *Sensitive to local minima*
- *Unstable slow convergence*

## ADVANTAGES:

- *Relatively simple*
- *Works for many parameters*



# Efficient adjoint gradient evaluation

Misfit function ( $F$ ) is normally defined using the forward problem solution ( $x$ ):

$$F(x, x(p))$$

Introducing residual and Jacobian of the forward problem:

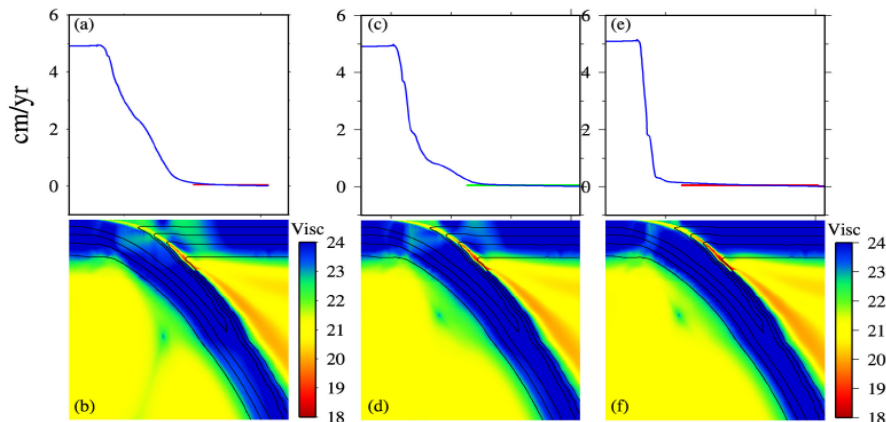
$$R(x) = 0 \quad J = \frac{\partial R}{\partial x}$$

we can efficiently evaluate the gradient using the adjoint method:

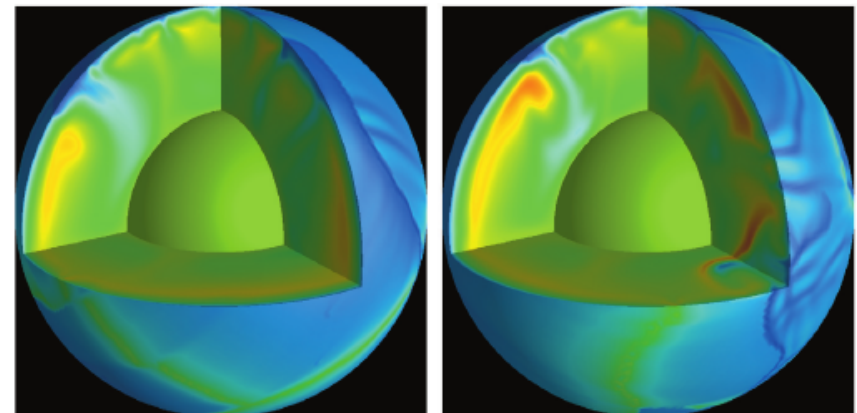
$$G = -\psi^T \frac{\partial R}{\partial p} \quad \psi = J^{-T} \left( \frac{\partial F}{\partial x} \right)^T$$

which only additionally requires evaluating the derivatives  $\frac{\partial R}{\partial p}$  and  $\frac{\partial F}{\partial x}$

Widely used technique in geodynamic model community (but not only), e.g.:



Ratnaswamy et al., 2015



Bunge et al., 2003

# Adjoint gradients explained

Objective function, formulated in terms of forward problem solution ( $x$ )

$$F(x, x(p))$$

Minimization (optimization, inversion)

Find input parameters ( $p$ ) such that  $F$  assumes minimum (preferably global) value

$$\min_p (F(x, x(p)))$$

Gradient-based methods (steepest descend, BFGS) require calculating the gradient of the objective function w.r.t input parameters

$$G = \frac{dF}{dp}$$

**LIMITATION!** Gradient methods are not suitable for finding global minima.

# Gradient of objective function

How do we get gradient? Just use chain rule!

$$G = \frac{dF}{dp} = \frac{\partial F}{\partial p} + \frac{\partial F}{\partial x} \frac{dx}{dp}$$

$$\frac{\partial F}{\partial p}$$

- Easy term (assumed to be zero in what follows)

$$\frac{\partial F}{\partial x}$$

- Easy term (objective function is usually directly expressed in terms of forward problem solution)

$$\frac{dx}{dp}$$

- difficult term (so-called (flow) sensitivity parameters)  
**ONE OF THE MAJOR LIMITATIONS OF ADJOINT METHOD**

x should be smooth and differentiable function of p. For certain rheology types (DP plasticity) it is not the case.

# Sensitivity parameters

How to get  $dx/dp$ ? Use chain rule once again plus an observation!

$$R(x) = 0 \quad - \text{residual of the forward problem}$$

$$\frac{dR}{dp} = \frac{\partial R}{\partial p} + \frac{\partial R}{\partial x} \frac{dx}{dp} \quad - \text{derivative of the residual (chain rule)}$$

$$\frac{dR}{dp} = 0 \quad - \text{why is that? Simple: forward problem residual must be zero for any set of input parameters. MAJOR TRICK!}$$

$$\frac{\partial R}{\partial x} = J \quad - \text{Jacobian matrix}$$

$$\frac{dx}{dp} = -J^{-1} \frac{\partial R}{\partial p} \quad - \text{solve for sensitivity parameters. VERY EXPENSIVE! (requires one linear solve with Jacobian per input parameter)}$$

# Adjoint system

How to make it less expensive?

$$G = \frac{\partial F}{\partial x} \frac{dx}{dp} = -\frac{\partial F}{\partial x} J^{-1} \frac{\partial R}{\partial p}$$

- plug dx/dp into gradient expression

$$\psi = J^{-T} \left( \frac{\partial F}{\partial x} \right)^T$$

- solve adjoint system. CHEAP! Requires only one solve, but with Jacobian transpose (adjoint)

$$G = -\psi^T \frac{\partial R}{\partial p}$$

- evaluate gradient (check by plugging psi)

$$(AB)^T = B^T A^T$$

$$(A)^{-T} = (A^T)^{-1} = (A^{-1})^T$$

The major advantage of adjoint method is that it requires only one linear solve per gradient evaluation. The disadvantage is that this solve involves Jacobian transpose. Symmetric cases are insensitive, but certain rheology types (DP plasticity) and discretizations (FDSTAG) are sensitive.



# Residual derivatives

The only remaining term is the derivative of forward problem residual:

$$\frac{\partial R}{\partial p}$$

For each new type of the input parameter (e.g. density, power-law exponent) it can be obtained by directly differentiating the residual expressions.

Alternatively one can use finite differences (for each input parameter):

$$\frac{\partial R}{\partial p_i} = \frac{R(p + e_i h) - R(p)}{h}$$

The derivatives are normally very sparse vectors, since only limited number of residual components are affected by each input parameter.

Irrespective of the evaluation method, one should utilize the sparsity.

# Adjoint scaling law

Scaling law relates change in the observable with the change in the solution parameter.

Consider general multi(two)-parametric scaling law:

$$q = a x^b y^c$$

Exponents can be determined separately by taking derivatives:

$$\frac{\partial q}{\partial x} = a b x^{b-1} y^c = \frac{b q}{x}$$

Which can be rearranged as (provided that gradients are known):

$$b = \frac{\partial q}{\partial x} \frac{x}{q}$$

We can view the observable (q) as an objective function and compute adjoint gradients!

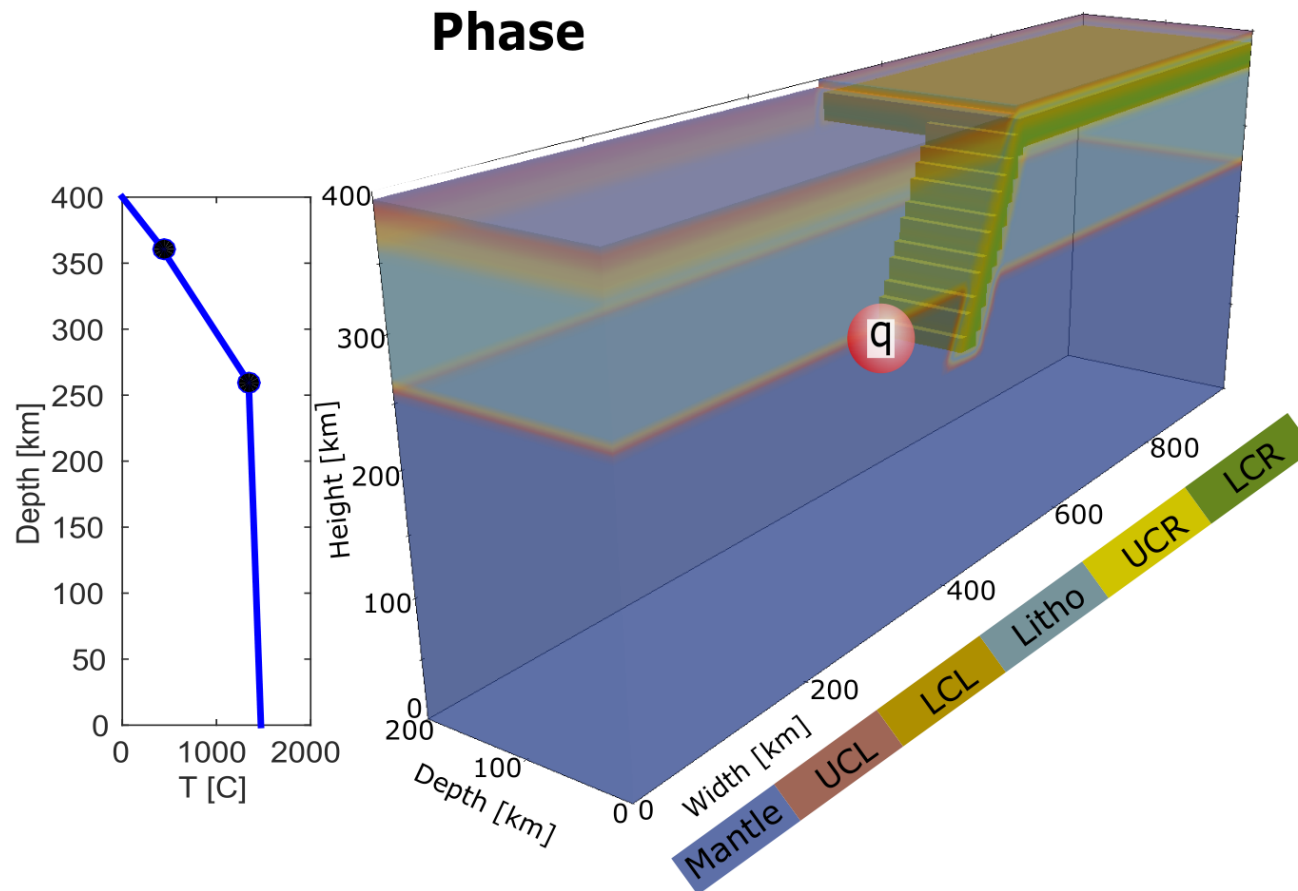
The remaining step is finding the prefactor:

$$a = \frac{q}{x^b y^c}$$

# 3D subduction synthetic test

Adjoint gradient evaluation is implemented in LaMEM (Reuber et al., in preparation)  
LaMEM is integrated with TAO package (Toolkit for Advanced Optimization)

More info is on poster of Georg Reuber

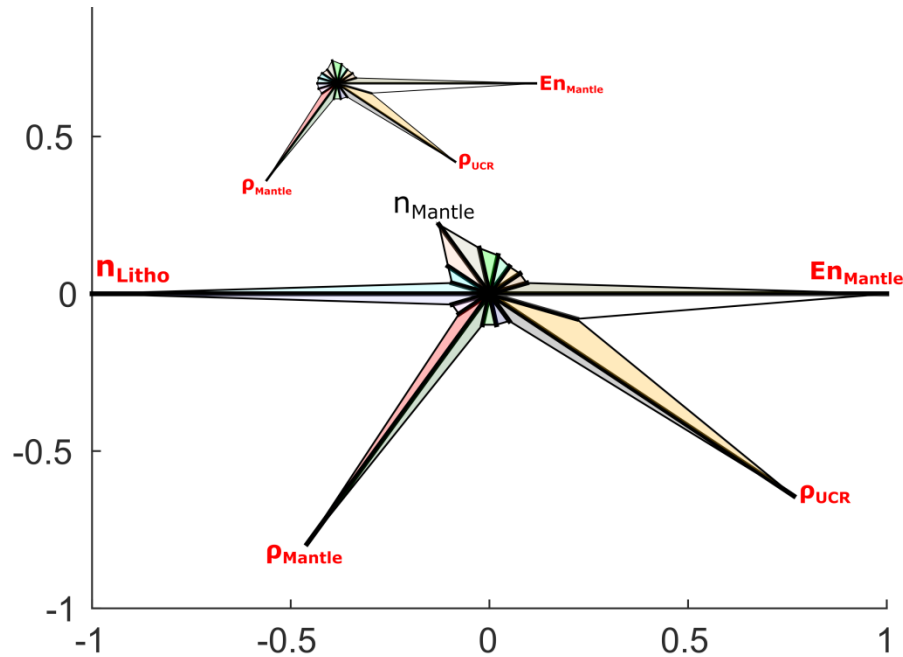


Growth rate at point q is an observable.

Activation energy and power law exponent are the scaling law parameters.

# Adjoint scaling law result

Normalized polar plot of scaling law exponents



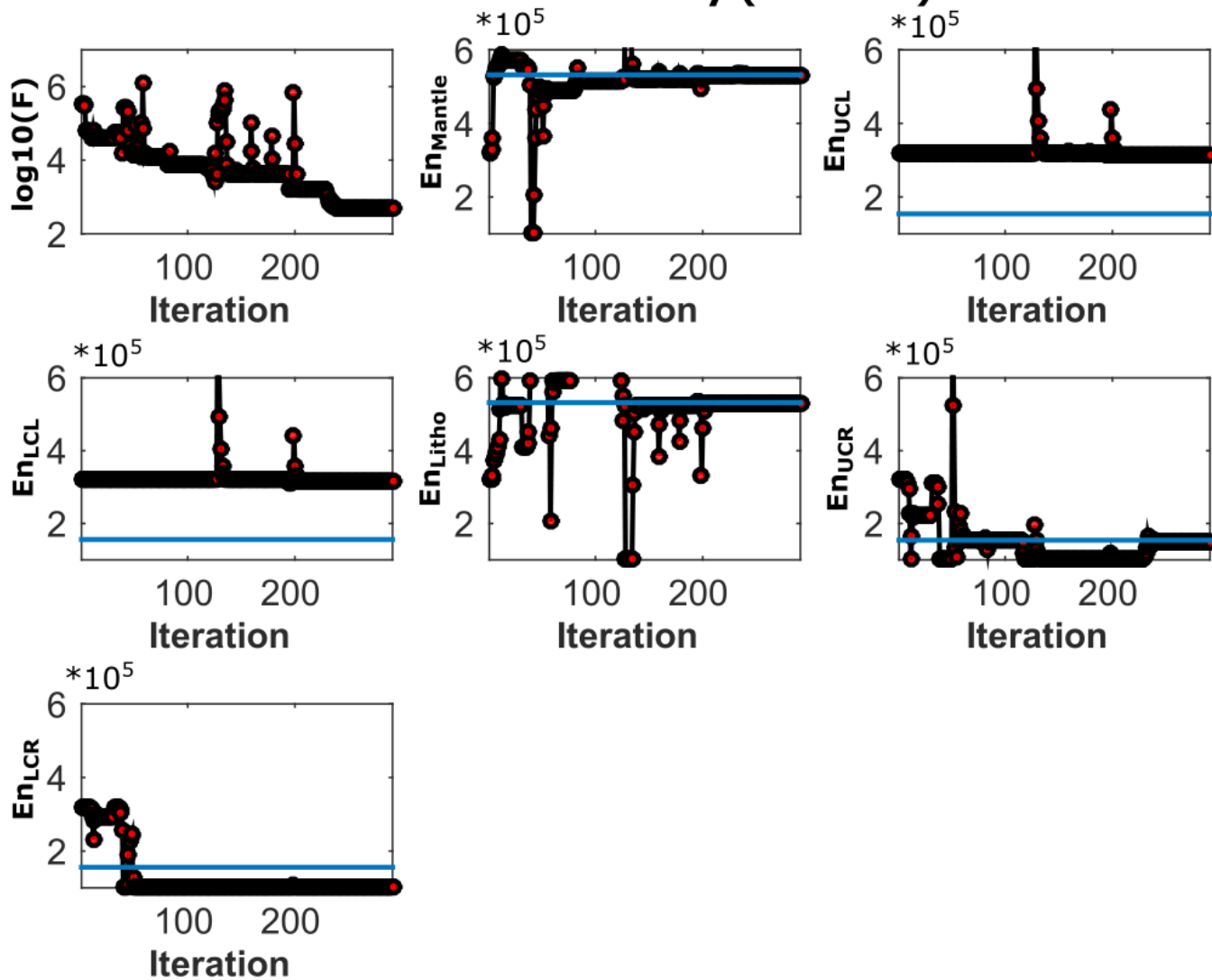
## Scaling law

$$9.5 = 6.3e123 * 532000^{-18.2} * 154000^0 * 156000^0 * 532000^{-1} * 154000^{-2.2} * 256000^{-2.7} * 2.3^0 * 2.4^0 * 3.5^0 * 2.3^0 * 2.4^0 * 3300^{13} * 2700^{-5e-4} * 3400^{-0.004} * 3300^{1.1} * 2700^{-14} * 3400^{3.3}$$

$$q = x * En_{Mantle}^a * En_{UCL}^b * En_{LCL}^c * En_{Litho}^d * En_{UCR}^e * En_{LCR}^f * n_{UCL}^g * n_{LCL}^h * n_{Litho}^i * n_{UCR}^j * n_{LCR}^k * \rho_{Mantle}^l * \rho_{UCL}^m * \rho_{LCL}^n * \rho_{Litho}^o * \rho_{UCR}^p * \rho_{LCR}^q$$

# Adjoint inversion result

## Inversion summary (Guess 1)



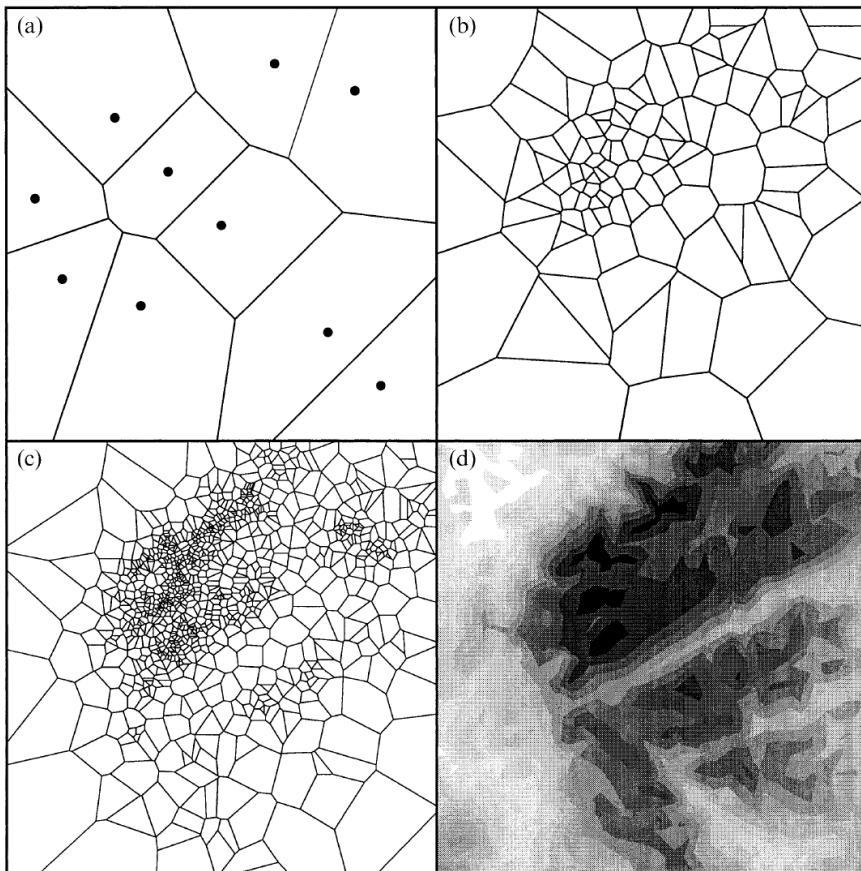
Inversion results for 3D subduction test.  
Not all the solution parameters are correctly inverted.  
Gradient-based methods are non-unique!

# Neighborhood algorithm (NA) (Sambridge, 1999)

Similar to simulated annealing, genetic and Monte-Carlo algorithms

Builds piecewise-constant Voronoi interpolant of the misfit function

Refines by performing a uniform random walk within lowest misfit cells



Sambridge, 1999

## ADVANTAGES:

- *Derivative-free*
- *Samples misfit function*
- *Attempts to identify multiple minima*

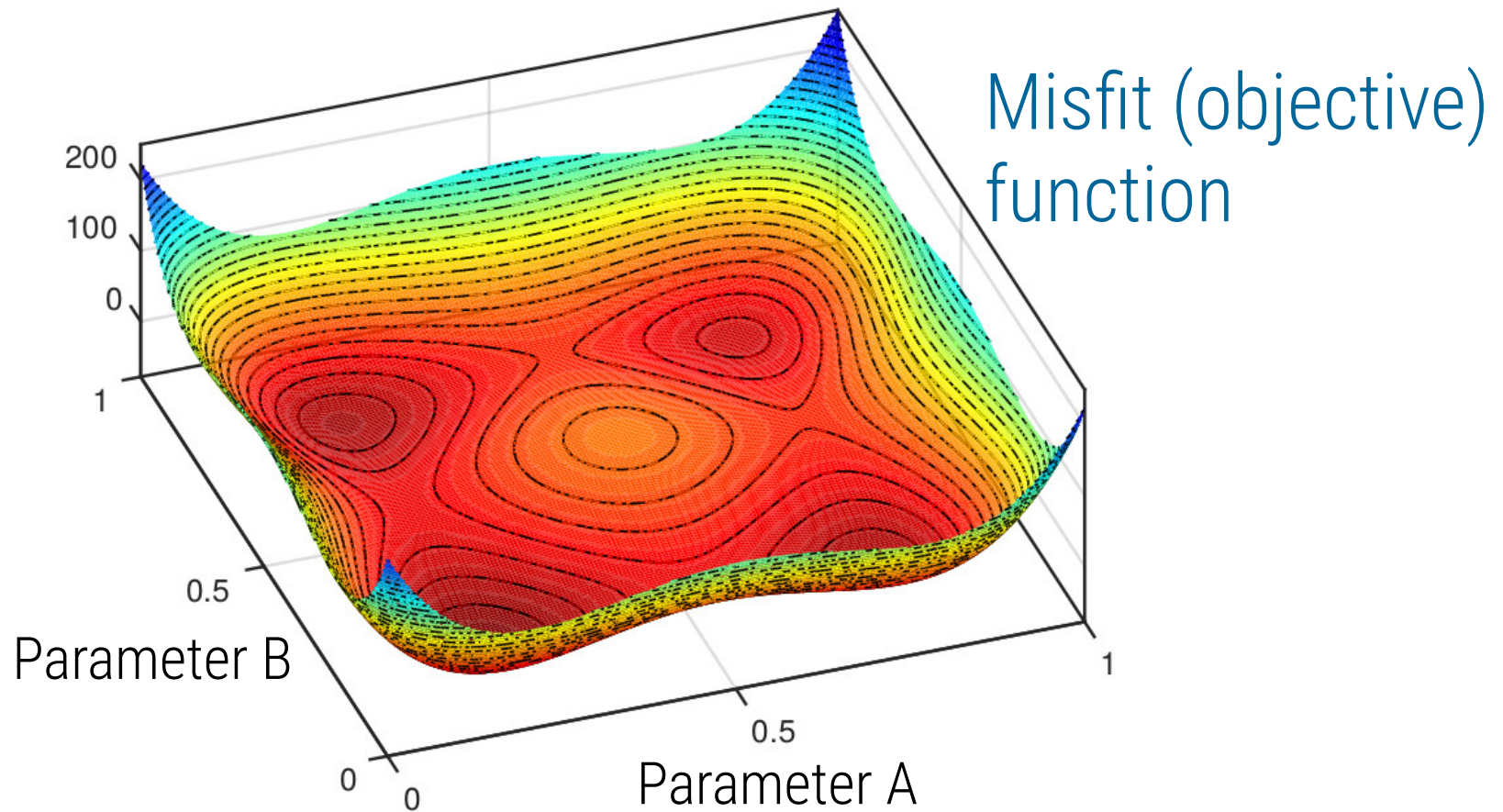
## DISADVANTAGES:

- *Requires many forward models*
- *Limited number of parameters*

# Neighborhood algorithm

Smarter sampling than Monte Carlo: **The Neighborhood Algorithm**

(original: Sambridge, 1999, extended parallel version: Baumann et al. 2014)

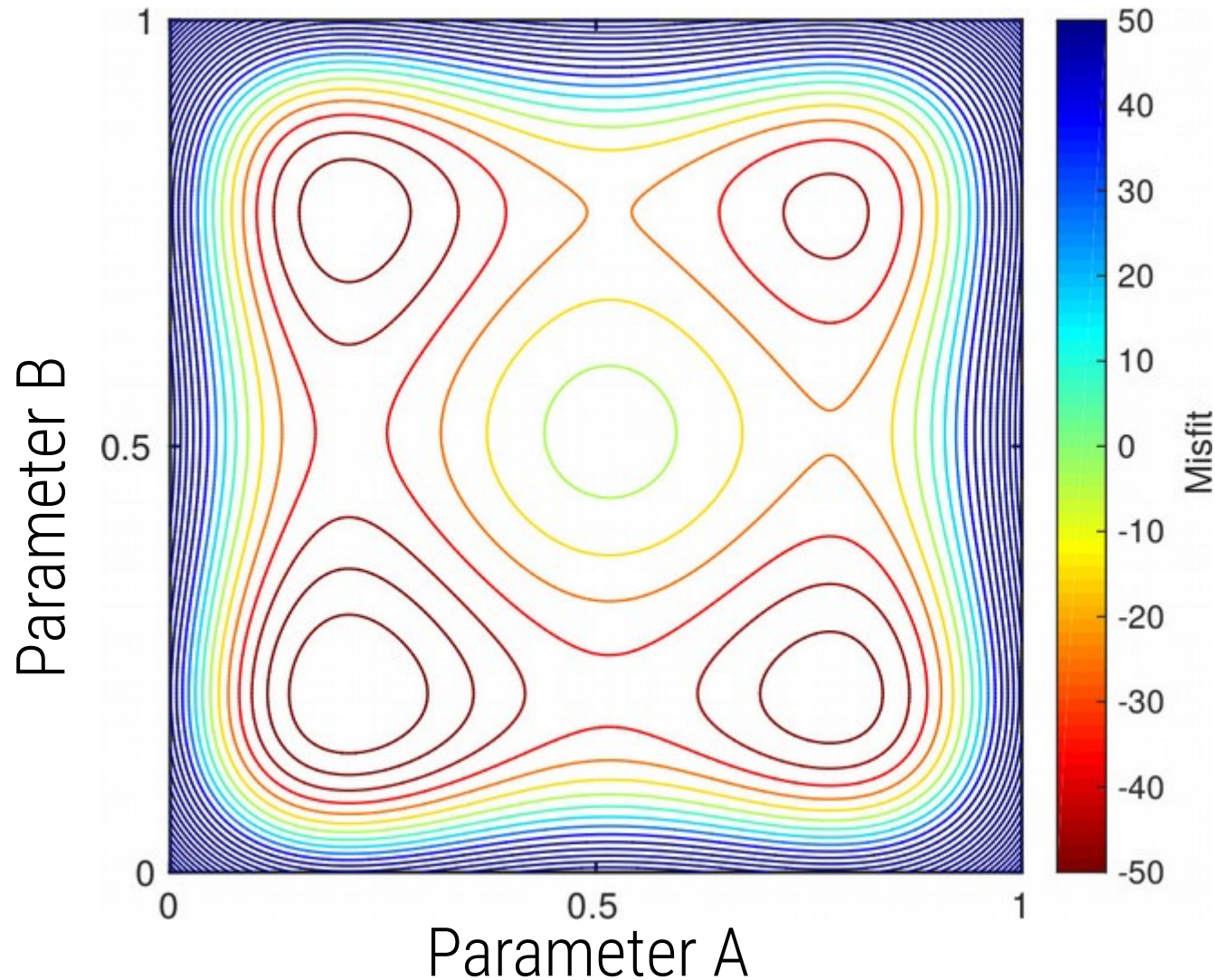




# Neighborhood algorithm

Smarter sampling than Monte Carlo: **The Neighborhood Algorithm**

(original: Sambridge, 1999, extended parallel version: Baumann et al. 2014)

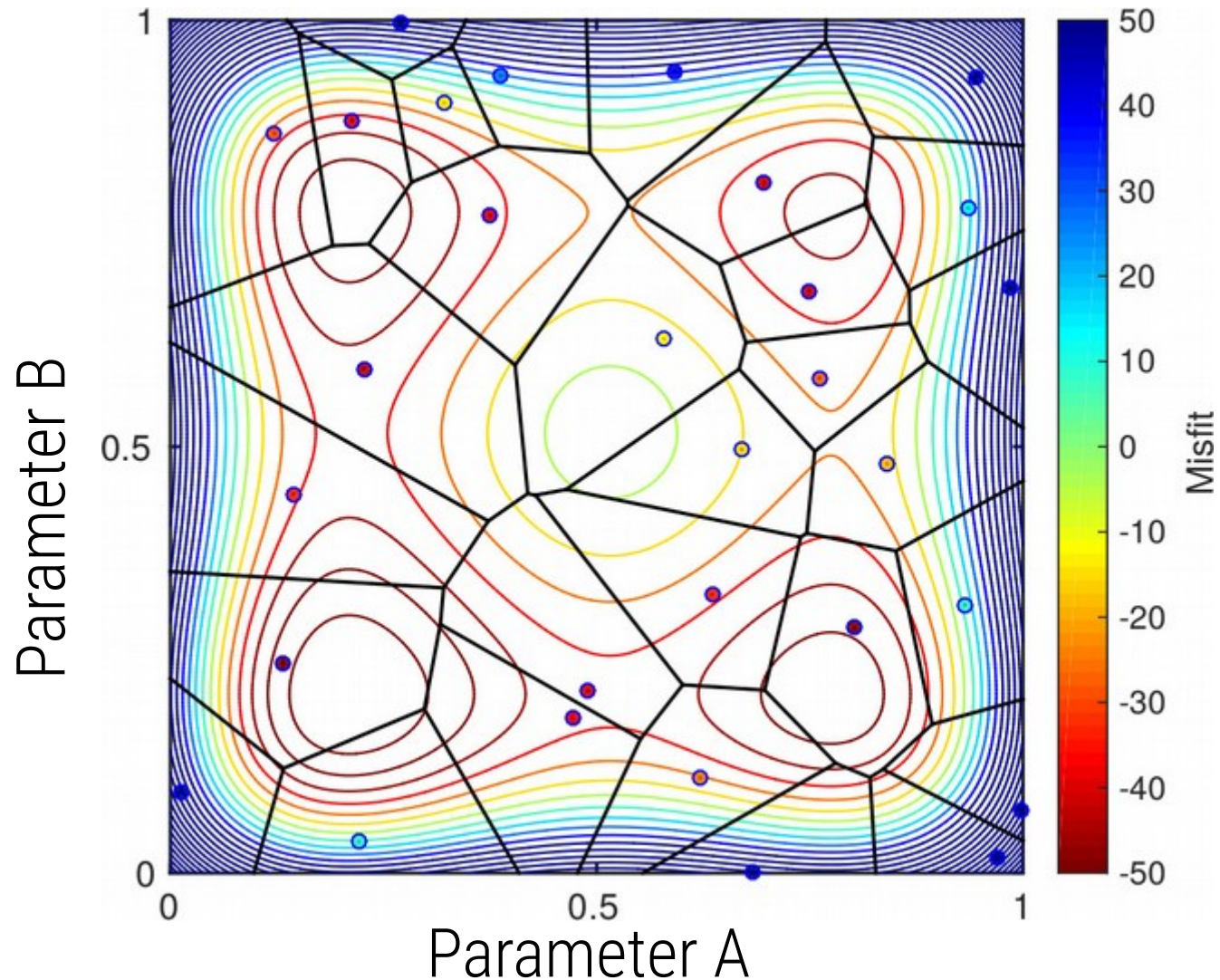




# Neighborhood algorithm

Smarter sampling than Monte Carlo: **The Neighborhood Algorithm**

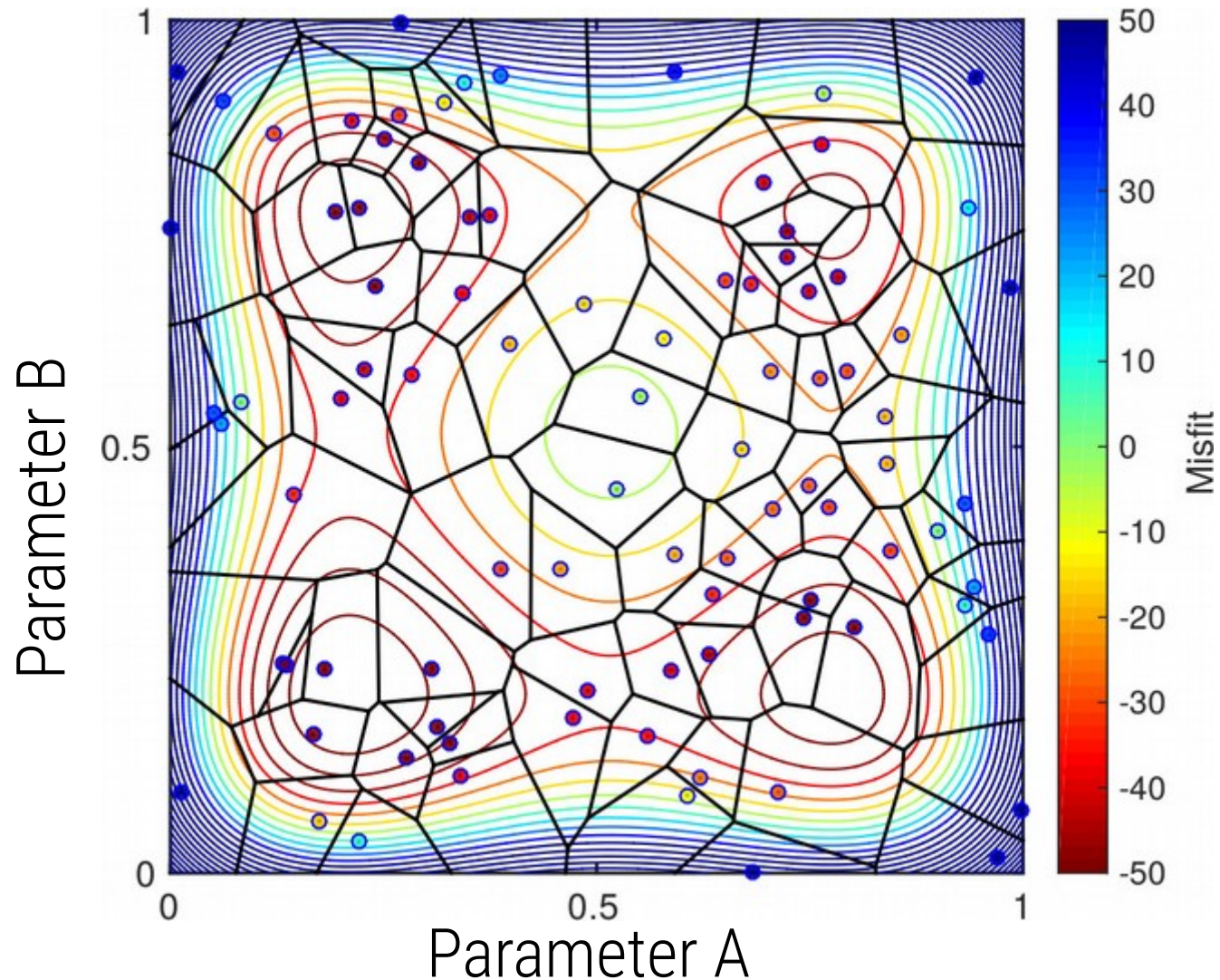
(original: Sambridge, 1999, extended parallel version: Baumann et al. 2014)



# Neighborhood algorithm

Smarter sampling than Monte Carlo: **The Neighborhood Algorithm**

(original: Sambridge, 1999, extended parallel version: Baumann et al. 2014)

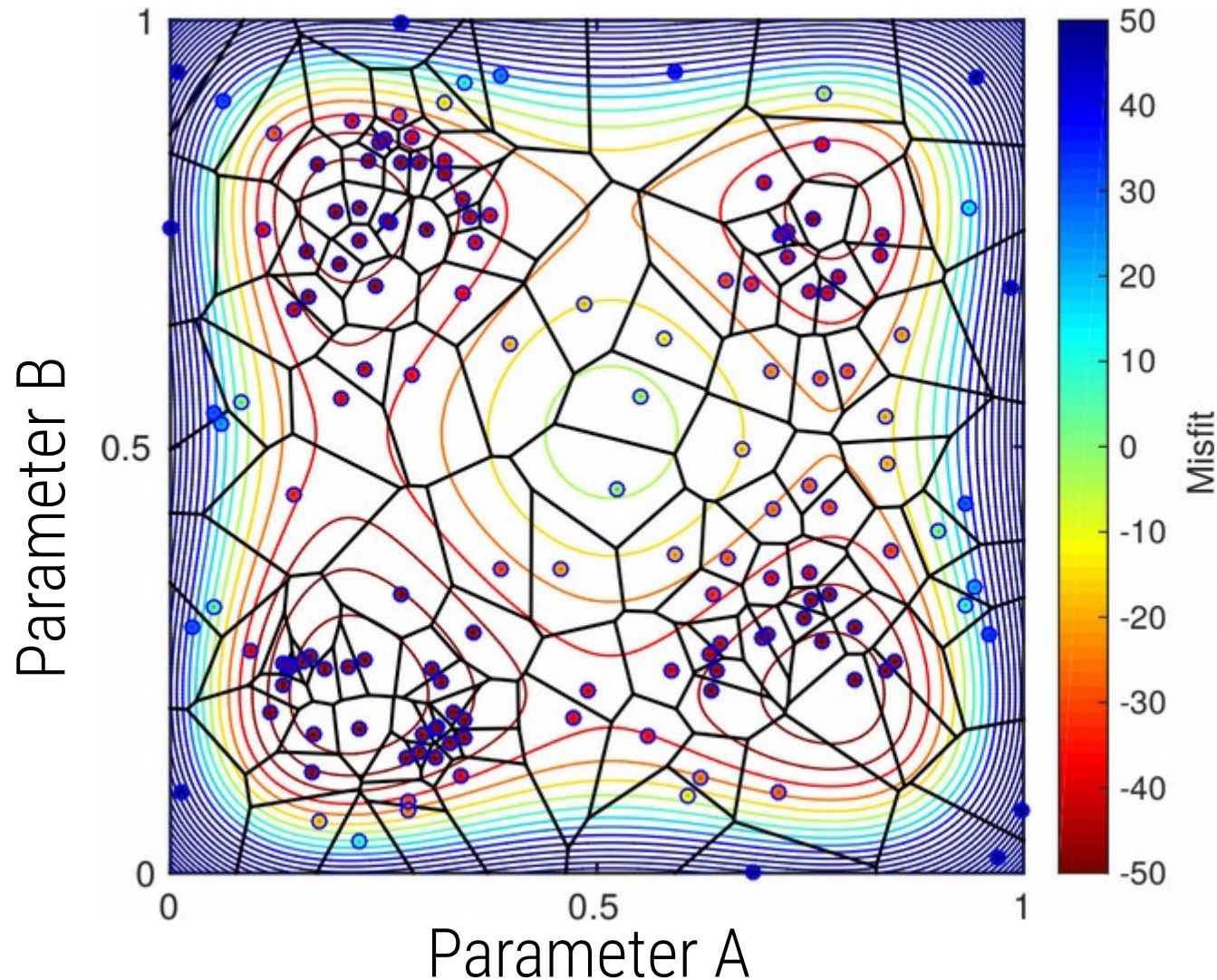




# Neighborhood algorithm

Smarter sampling than Monte Carlo: **The Neighborhood Algorithm**

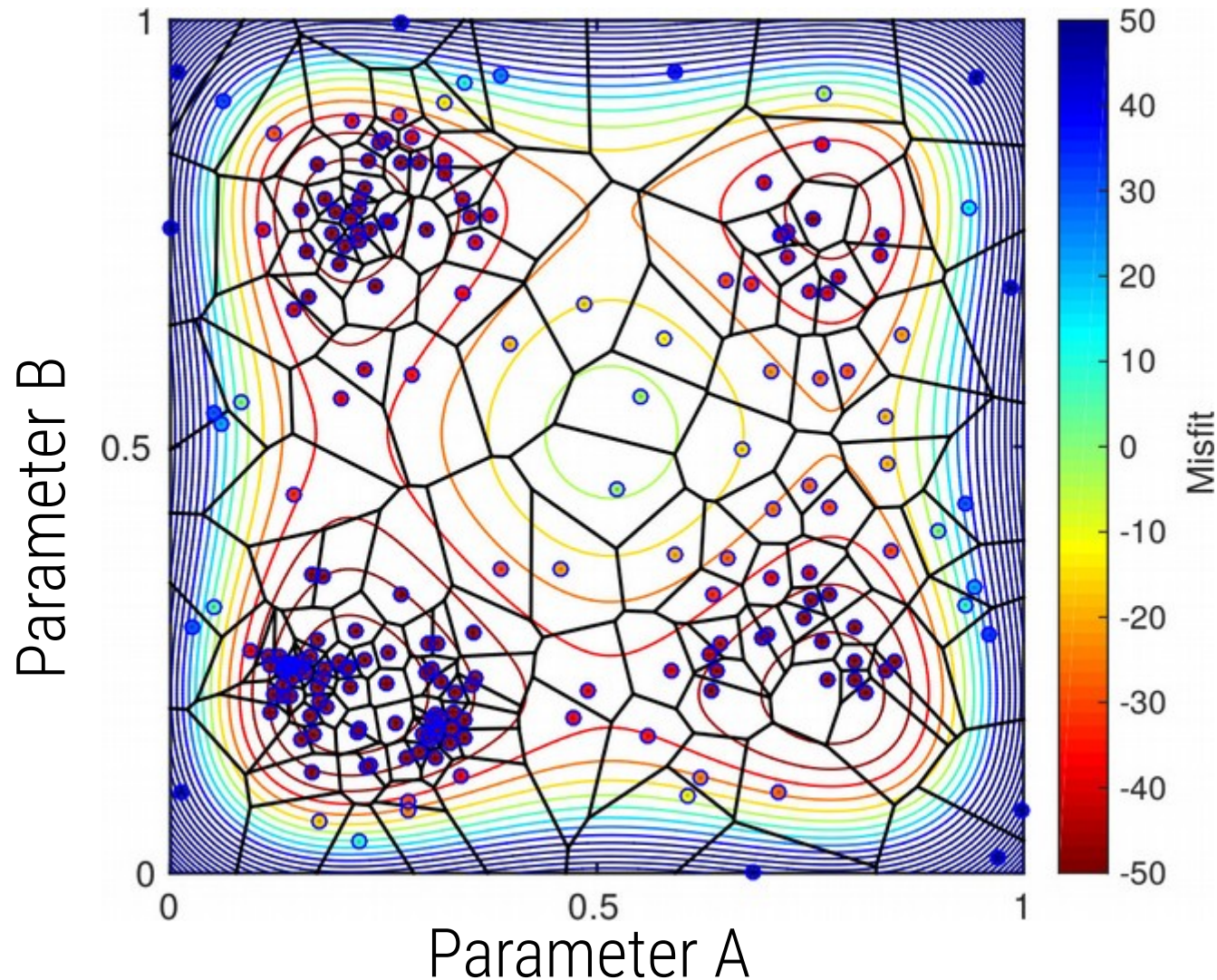
(original: Sambridge, 1999, extended parallel version: Baumann et al. 2014)



# Neighborhood algorithm

Smarter sampling than Monte Carlo: **The Neighborhood Algorithm**

(original: Sambridge, 1999, extended parallel version: Baumann et al. 2014)

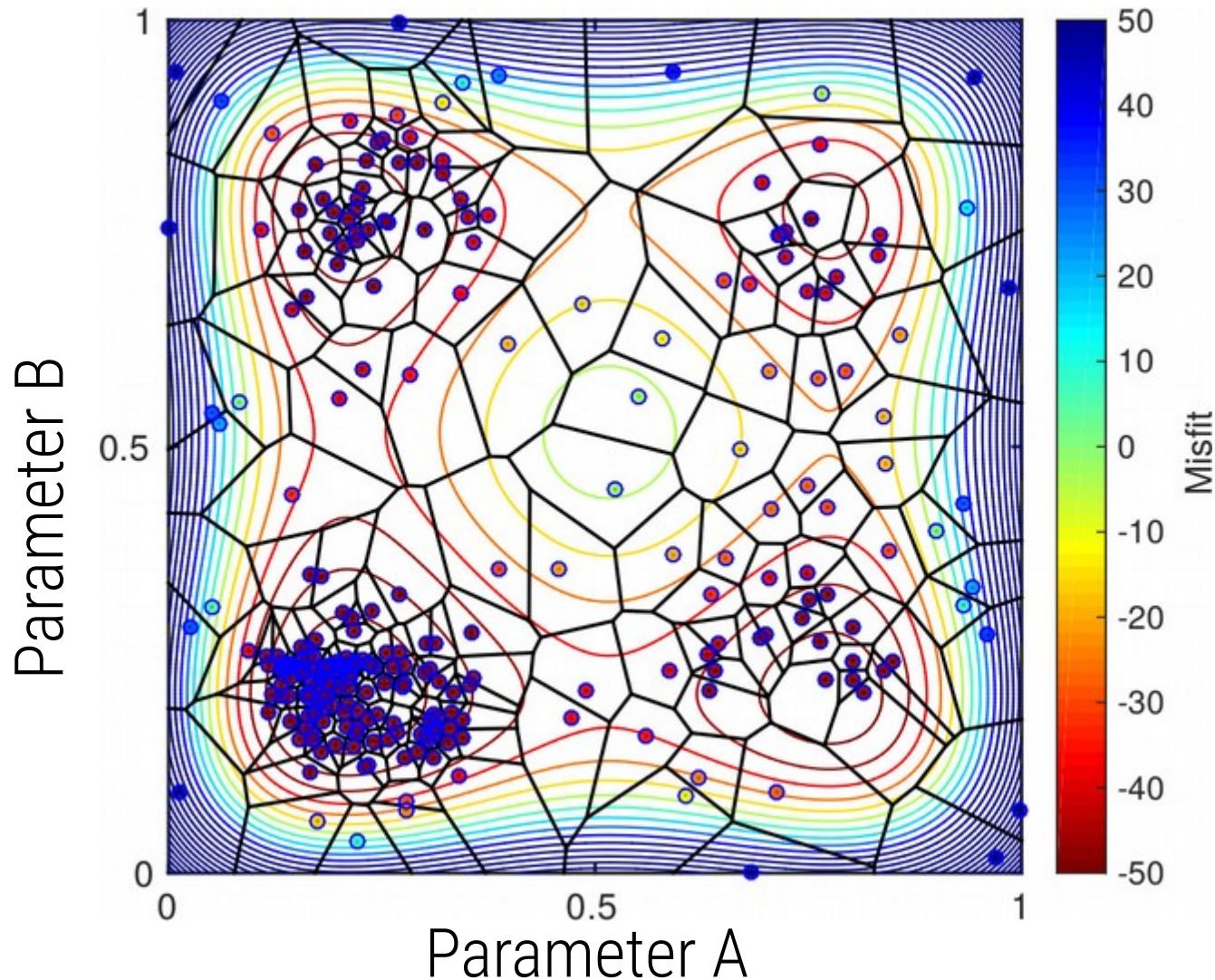




# Neighborhood algorithm

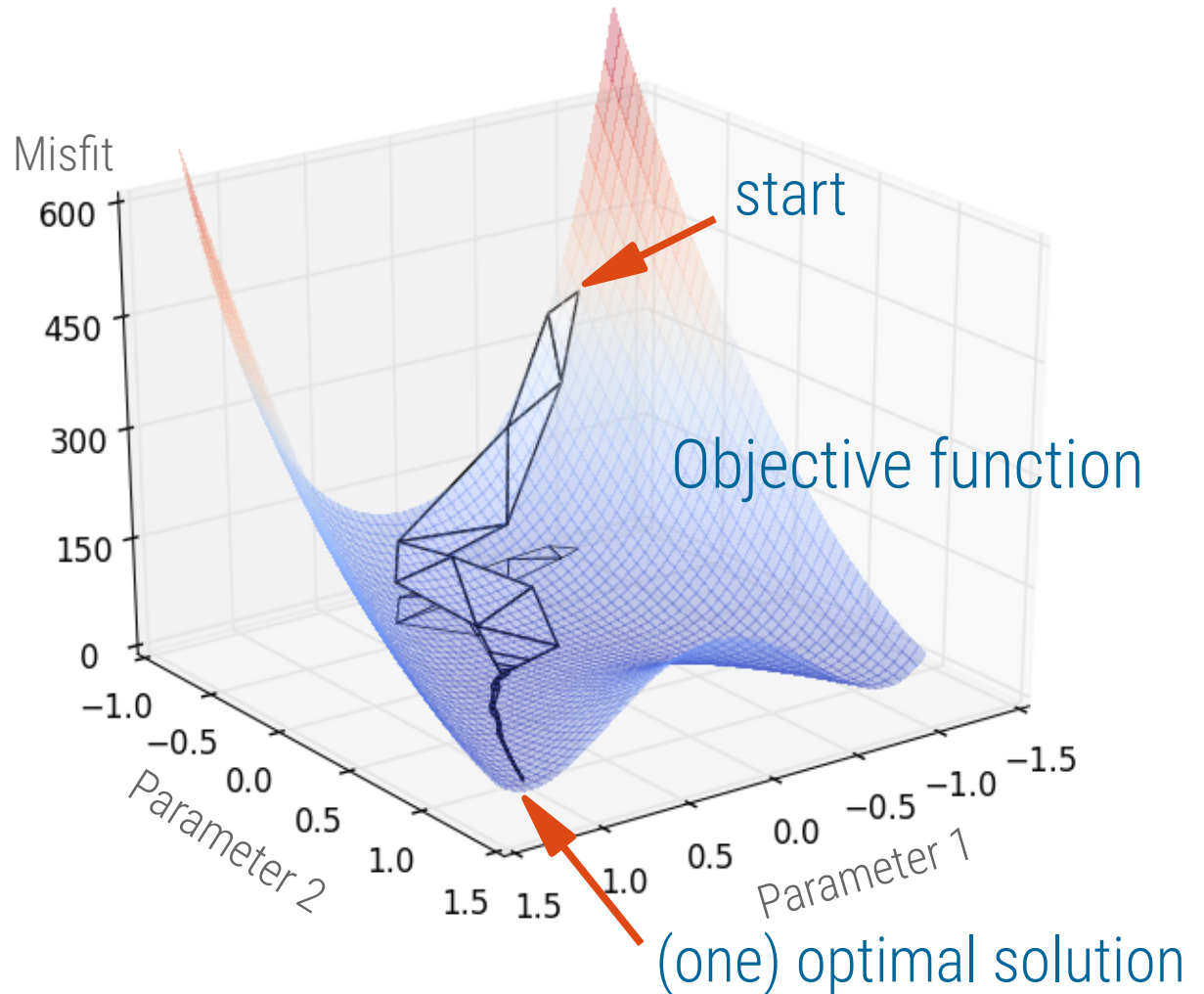
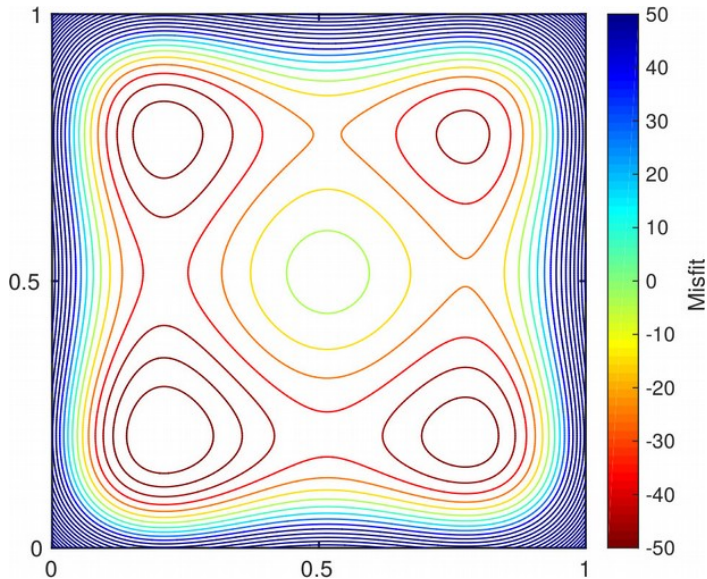
Smarter sampling than Monte Carlo: **The Neighborhood Algorithm**

(original: Sambridge, 1999, extended parallel version: Baumann et al. 2014)



# Downhill Simplex Method (Nelder & Mead 1965)

- Integrated with LaMEM using TAO package
- Always replace worst vertex of simplex
  - High dimensions





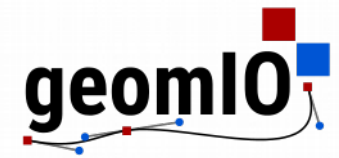
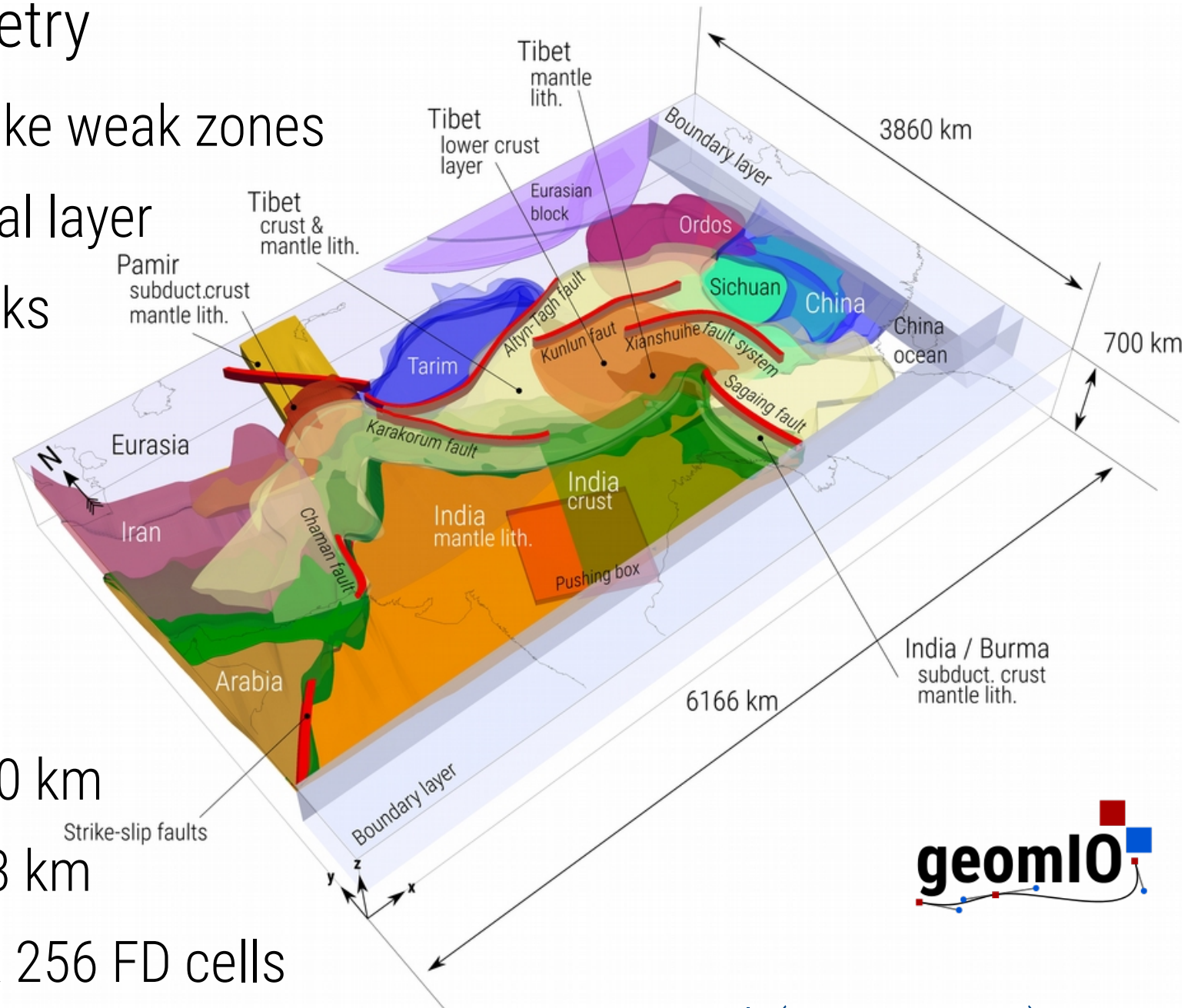
# 3D India-Asia collision

- Model geometry

- Strike-slip like weak zones
- Weak crustal layer
- Strong blocks
- Slabs

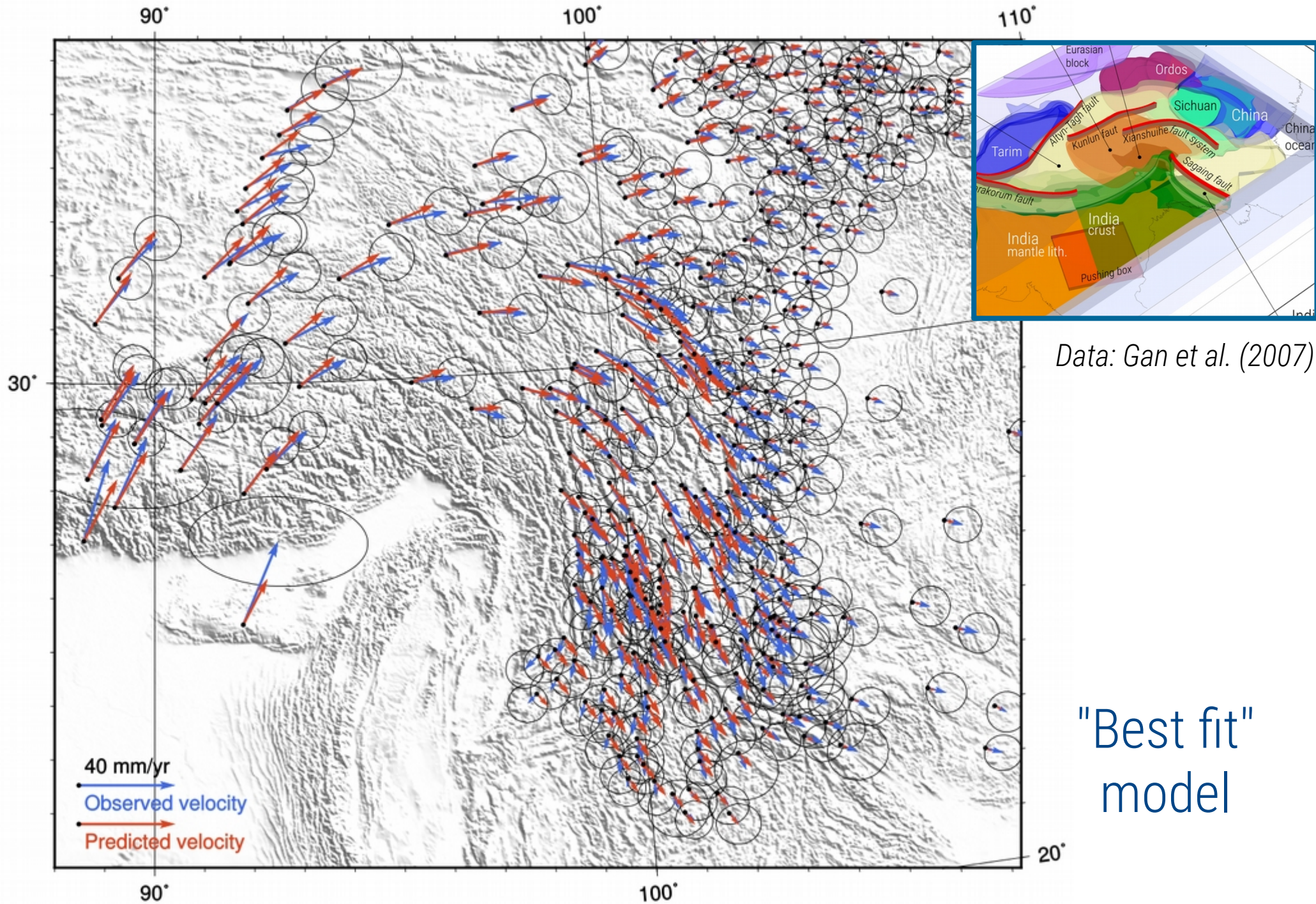
- Resolution

- Lateral: 7-10 km
- Vertical: 2-3 km
- 512 x 512 x 256 FD cells





# 3D India-Asia collision





# 3D India-Asia collision

"Best fit"  
model

